CRISPR/Cas-mediated non-viral genome specific targeted CAR T cells achieve high safety and efficacy in relapsed/refractory B-cell non-Hodgkin lymphoma

He Huang (huanghe@zju.edu.cn)
The First Affiliated Hospital, School of Medicine, Zhejiang University https://orcid.org/0000-0002-2723-1621

Jiqin Zhang
East China Normal University

Yongxian Hu
The First Affiliated Hospital, School of Medicine, Zhejiang University

Jiaxuan Yang
Shanghai Research Center for Gene Editing and Cell Therapy, Shanghai Key Laboratory of Regulatory Biology, School of Life Sciences, East China Normal University, Shanghai, China

Wei Li
Bioray Laboratories Inc., Shanghai, China

Mingming Zhang
Bone Marrow Transplantation Center, The First Affiliated Hospital, School of Medicine, Zhejiang University, Hangzhou, Zhejiang, China

Yue Tian
Shanghai Research Center for Gene Editing and Cell Therapy, Shanghai Key Laboratory of Regulatory Biology, School of Life Sciences, East China Normal University, Shanghai, China

Guoqing Wei
Bone Marrow Transplantation Center, The First Affiliated Hospital, School of Medicine, Zhejiang University, Hangzhou, Zhejiang, China

Linjie Zhang
Shanghai Research Center for Gene Editing and Cell Therapy, Shanghai Key Laboratory of Regulatory Biology, School of Life Sciences, East China Normal University, Shanghai, China

Kui Zhao
PETCT Center, The First Affiliated Hospital, School of Medicine, Zhejiang University, Hangzhou, Zhejiang, China

Binghe Tan
Shanghai Research Center for Gene Editing and Cell Therapy, Shanghai Key Laboratory of Regulatory Biology, School of Life Sciences, East China Normal University, Shanghai, China

Jiazhen Cui
Bone Marrow Transplantation Center, The First Affiliated Hospital, School of Medicine, Zhejiang University, Hangzhou, Zhejiang, China
Yalei Qi
Shanghai Research Center for Gene Editing and Cell Therapy, Shanghai Key Laboratory of Regulatory Biology, School of Life Sciences, East China Normal University, Shanghai, China
Yi Li
Bone Marrow Transplantation Center, The First Affiliated Hospital, School of Medicine, Zhejiang University, Hangzhou, Zhejiang, China
Qiliang Tian
Bioray Laboratories Inc., Shanghai, China
Qingcan Wang
Bioray Laboratories Inc., Shanghai, China
Yuxuan Wu
Shanghai Research Center for Gene Editing and Cell Therapy, Shanghai Key Laboratory of Regulatory Biology, School of Life Sciences, East China Normal University, Shanghai, China
Dali Li
Shanghai Key Laboratory of Regulatory Biology East China Normal University https://orcid.org/0000-0002-0046-8493
Bing Du
Shanghai Research Center for Gene Editing and Cell Therapy, Shanghai Key Laboratory of Regulatory Biology, School of Life Sciences, East China Normal University, Shanghai, China
Mingyao Liu
East China Normal University

Biological Sciences - Article

Keywords: non-Hodgkin lymphoma, chimeric antigen receptor (CAR) T cell therapy

Posted Date: April 3rd, 2021

DOI: https://doi.org/10.21203/rs.3.rs-373651/v1

Version of Record: A version of this preprint was published at Nature on August 31st, 2022. See the published version at https://doi.org/10.1038/s41586-022-05140-y.

CRISPR/Cas-mediated non-viral genome specific targeted CAR T cells achieve high safety and efficacy in relapsed/refractory B-cell non-Hodgkin lymphoma

Jiqin Zhang[1,3,8], Yongxian Hu[2,4,5,6,8], Jiaxuan Yang[1,8], Wei Li[3], Mingming Zhang[2,4,5,6], Yue Tian[1], Guoqing Wei[2,4,5,6], Linjie Zhang[1], Kui Zhao[7], Binghe Tan[1,3], Jiazhen Cui[2,4,5,6], Yalei Qi[1], Yi Li[2,4,5,6], Qiliang Tian[3], Qingcan Wang[3], Yuxuan Wu[1], Dali Li[1], Bing Du[1,✉], Mingyao Liu[1,✉], He Huang[2,✉]

[1]Shanghai Research Center for Gene Editing and Cell Therapy, Shanghai Key Laboratory of Regulatory Biology, Institute of Biomedical Sciences and School of Life Sciences, East China Normal University, Shanghai, China

[2]Bone Marrow Transplantation Center, The First Affiliated Hospital, School of Medicine, Zhejiang University, Hangzhou, Zhejiang, China

[3]Bioray Laboratories Inc., Shanghai, China

[4]Zhejiang Province Engineering Laboratory for Stem Cell and Immunity Therapy, Hangzhou, China;

[5]Institute of Hematology, Zhejiang University, China, Hangzhou, China;

[6]Zhejiang Laboratory for Systems & Precision Medicine, Zhejiang University Medical Center, Hangzhou, China;

[7]PETCT Center, The First Affiliated Hospital, School of Medicine, Zhejiang University, Hangzhou, Zhejiang, China

[8]These authors contributed equally

✉e-mail: bdu@bio.ecnu.edu.cn; myliu@bio.ecnu.edu.cn; huanghe@zju.edu.cn

Abstract

In recent years, chimeric antigen receptor (CAR) T cell therapy has shown great promise in treating hematological malignancies. However, CAR T cell therapy currently has several limitations. Here we successfully developed a two-in-one approach to generate non-viral genome specific targeted CAR T cells through CRISPR/Cas9. Based on the optimized protocol, the feasibility was preliminarily demonstrated by a preclinical study inserting an anti-CD19 CAR cassette into the *AAVS1* safe harbor locus. We found that non-viral *AAVS1*-knockin CAR T cells behave comparably to those conventionally produced by lentivirus. Furthermore, an innovative type of anti-CD19 CAR T cells with *PD1*-integration was constructed and shows a superior ability to eradicate tumor cells with high PD-L1 expression. In adoptive therapy for relapsed/refractory (r/r) aggressive B-cell non-Hodgkin lymphoma (B-NHL), we observed a high rate (87.5%) of complete remission (CR) and durable responses without serious adverse events in eight patients after treatment. Notably, these enhanced CAR T cells were effective even at a low infusion dose and with a low CAR percentage, which indicated that they have higher potency. No off-target events were found in the infusion product. Single-cell RNA sequencing analysis further validated the advantage of PD1 interference that results in fewer dysfunctional CAR T cells through this treatment. Collectively, our results demonstrate the outstanding safety and efficacy of non-viral genome specific integrated CAR T cells, thus providing a revolutionary technology for CAR T cell therapy.

Introduction

In recent years, CAR T cell therapy has rapidly developed and shows a great potential in cancer therapy, which is exemplified by the FDA approval of four anti-CD19 CAR T cell treatments[1-5]. Nevertheless, there still remain some limitations, including the complicated manufacturing process, high production cost, long preparation time and potential safety concerns of current therapies. The use of virus in CAR T cell production is one area of concern, as the disadvantages include that insertional

mutagenesis increases the risk of tumor development[6,7]. Furthermore, specific responses to virus-derived DNA tend to impede CAR expression[8,9] and virus manufacture frequently incurs high costs[10]. Although some strategies, such as using transposon systems[11-14] and mRNA transduction[15,16], are being exploited to generate CAR T cells without virus, the low homogeneity of final products caused by random integration and discontinued CAR expression become additional problems. Recently, several studies have shown that CRISPR/Cas9 technology can be applied to generate locus specific integrated CAR T cells by using an adeno-associated virus (AAV) vector as a template[17,18]. Furthermore, one preferential non-viral strategy was proposed to produce T cell products with point mutation correction and precise insertion of the TCR element[19]. Thus, in order to simultaneously solve the disadvantages of virus usage and random integration, here we further optimized the conditions and developed non-viral genome specific targeted CAR T cells through CRISPR/Cas9. The feasibility was preliminarily demonstrated by preclinical experiments using *AAVS1*-targeted anti-CD19 CAR T cells. Given that blockage of the PD1/PD-L1 pathway by inhibitors or gene editing has been reported to improve the antitumor activity of CAR T cells[20-23], we generated enhanced *PD1*-integrated anti-CD19 CAR T cells and demonstrated their safety and effectiveness in treating patients with r/r B-NHL.

Results

First, we sought to optimize the protocol for producing non-viral genome specific integrated T cells. It was found that a homology directed repair (HDR) template, in the form of linear double-stranded DNA (dsDNA), could achieve high recombination efficiency and cell viability (Figure 1a, S1a-c). More viable integrated cells were acquired when electroporation was carried out in stimulated T cells by applying 800bp homology arms (Figure 1b, c, S1d-g, S2). After confirmation of an optimal protocol, for proof of concept, we first chose to introduce the CAR targeting construct into the *AAVS1* safe harbor, which excludes the influence caused by functional endogenous genes, to evaluate whether this approach would affect the

properties of CAR T cells. An anti-CD19 CAR sequence was constructed, which was comprised of the intracellular domain of 4-1BB and CD3 ζ (named as 19bbz). The integration efficiency of 19bbz into *AAVS1* was about 10% (up to 19.80%) and the indel percentage ranged from 67% to 87% in healthy donor cells (Figure 1d, e, S3a). Also, the integration was unbiased between bulk $CD3^+$, $CD4^+$ and $CD8^+$ T cells (Figure S3b, c). To understand the influence caused by the method per se, we comprehensively compared *AAVS1*-integrated anti-CD19 CAR T cells (named as AAVS1-19bbz) with lentivirus-produced anti-CD19 CAR T cells (named as LV-19bbz). Although the electroporation procedure itself led to some cell damage, T cell expansion was not impaired and high cell viability was detected after thorough recovery (Figure S3d-f). Interestingly, electroporation manipulation conferred a growth advantage on $CD8^+$ T cells over $CD4^+$ cells when compared to lentivirus infection (Figure S3g), which was consistent with a previous study[19]. We observed that AAVS1-19bbz and LV-19bbz cells exhibited comparable cell expansion after tumor cell stimulation (Figure 1f, S3h). Our approach did not change the differentiation of T cell subsets (Figure S3i). In comparison to untreated T cells, AAVS1-19bbz cells responded to tumor cells as well as LV-19bbz did, with a little difference in cell marker expression and cytokine secretion (Figure 1g, h). Importantly, like LV-19bbz cells, AAVS1-19bbz cells vigorously eradicated tumor cells *in vitro* and *in vivo* (Figure 1i, j, S3j-l). Meanwhile, precise integration of the CAR cassette was validated by Sanger sequencing and non-targeted integration detection (Figure S4). Taken together, these results demonstrate that the strategy to produce non-viral genome specific targeted CAR T cells is feasible.

Due to the well-known inhibition of T-cell effector function through the PD1/PD-L1 pathway, we set out to develop an enhanced type of CAR T cells by integrating an anti-CD19 CAR sequence into the *PD1* gene (named as PD1-19bbz). CAR expression was detected in about 20% (up to 30.3%) of healthy donor T cells (Figure 2a, b). A high indel percentage (83%-93%) was observed in total T cells from five representative donors (Figure 2c). The impairment of PD1 in PD1-19bbz cells was demonstrated by low PD1 protein expression in CAR^+ cells after co-culture with

tumor cells (Figure 2d). PD1-19bbz cells had higher proliferation than LV-19bbz cells after repeated stimulation by PD-L1 expressing Raji cells (Figure 2e). As indicated by other reports[24-26], PD1 disruption did not affect the elevation of activation markers and cytokine secretion to counteract targeted tumor cells (Figure 2f, g). In contrast to LV-19bbz cells, PD1-19bbz cells showed more robust clearance of PDL1-upregulated tumor cells *in vitro* and *in vivo* (Figure 3h-j). Collectively, these data indicate that non-viral *PD1*-integrated CAR T cells have the potential to more effectively eliminate tumor cells.

Based on our preclinical experimental data, we then proceeded to carry out a phase I clinical trial to evaluate the safety and efficacy of PD1-19bbz cells in treating patients with r/r B-NHL (ClinicalTrials.gov NCT04213469). In the final infusion products of eight patients, the average percentages of CAR integration and *PD1* indel were about 20% and 60%, respectively (Figure S5a-d). The infusion products had a cell viability of more than 90%, and responded to and eradicated tumor target cells *in vitro* (Figure S5e-g). Next, we undertook whole genome sequencing (WGS) to detect off-target events in one representative infusion product. Exclusive indels in the edited sample, which located around 2,219 potential off-target sites predicted by Cas-OFFinder, were identified by bioinformatics and further validated by deep sequencing. As a result, no verified indels were found within 200bp upstream and downstream of these sites (Figure S6, Table S1). Indel events were also not detected at 29 top-ranked potential off-target sites predicted by the Benchling CRISPR tool, by using deep sequencing analysis (Table S2).

Eight patients were given a lymphodepleting chemotherapy regimen using combined cyclophosphamide and fludarabine, followed by one infusion of PD1-19bbz cells with a dose of 0.56×10^6-2.35×10^6 cells/kg body weight (Table 1, S3, S4). While all the patients experienced transient and reversible hematologic toxicity events mainly related to the chemotherapy pretreatment, no other high-grade (≥3) adverse events were found (Table S5). Mild cytokine release syndrome (CRS) was observed in some patients and no immune effector cell-associated neurotoxicity syndrome (ICANS) occurred (Figure 3a, S7). PD1-19bbz cells proliferated and persisted *in vivo*

(Figure 3b, c). While the peak of CAR T cell expansion in most patients was on day 7 to 14 after infusion, a slower changing curve was detected in one patient. During a median observation period of five months, CR was achieved in 7/8 (87.5%) patients as shown by positron emission tomography–computed tomography (PET-CT) scans and durable responses were found in all seven patients at the time of last follow-up (Figure 3d, e, Table 1). Partial remission (PR) was observed in the remaining (1/8) patient, thus the best objective response rate reached 100% in all the patients. Of note, PD1-19bbz cells effectively functioned even at a low infusion dose and with a low CAR percentage, thereby indicating high potency of these *PD1* knockout CAR T cells. Together, these data demonstrate that non-viral *PD1*-integrated CAR T cells have high safety and efficacy for patients with r/r B-NHL.

To further understand the characteristics of non-viral *PD1*-integrated CAR T cells before and after infusion, single-cell RNA sequencing (scRNA-seq) was carried out in three patient samples. After standard data processing and quality control procedures, transcriptomic profiles of 54,774 cells were obtained. Total cells were divided into five types using a graph-based clustering method (Figure S8) and the subtype of $CD8^+$ T cells was further analyzed (Figure S9). To unravel the features of infusion products, two clusters (C1, C2) were defined by using CD8 memory and dysfunction marker genes, and the expression of a wide range of memory, dysfunction and cytotoxicity genes[27-29] was analyzed (Figure 4a, S10b-h, Table S6). It was noteworthy that the percentage of the CD8 memory cluster was about 80% in mixed samples, and it even reached above 95% in two individual samples (Figure 4b). The proportion of C1 and C2 was similar between CAR^+ and CAR^- cells (Figure S10a, S11). Next, we set out to understand the kinetics of gene expression in $CD8^+/CAR^+$ cells through the treatment (Figure 4c). As expected, almost no expression of PD1 was detected in all the samples (Figure 4d, S10i). Intriguingly, like PD1, a series of dysfunction genes including BTLA, CD244, CD200, CD109, ENTPD1, LAYN and CXCL13 maintained very low expression as well (Figure 4d, Table S7-S9), which was in line with the previous findings[30,31]. Additionally, sustained expression of memory genes and attenuated expression of dysfunction genes were found in CAR^+

cells after infusion into patients (Figure 4e-f, S12, S13, Table S7-S9), thereby suggesting that PD1-19bbz cells had a lower tendency to become exhausted *in vivo*. The activities of different pathways were also analyzed in the samples (Figure S14). Altogether, these scRNA-seq data reveal more memory and fewer dysfunctional CAR^+ cells in pre-infused and post-infused PD1-19bbz cells, thus giving a mechanistic explanation for their superior efficacy in the clinical trial.

Discussion

CRISPR/Cas9-mediated HDR is becoming a usual method to facilitate precise integration of target sequences[32-34]. Recently, one study showed the feasibility of editing human T cells using a non-viral genome targeting strategy[19]. Here, we further optimized the protocol to achieve higher recombination efficiency and thus generated genome specific targeted CAR T cells without using virus. Despite a relatively low percentage of CAR^+ cells in comparison to lentivirus-produced CAR T cells, we substantiate that non-viral genome specific integrated CAR T cells are effective and an additional enrichment step is unnecessary for clinical application. In addition, although the electroporation step results in some cell damage, our data indicate that T cell expansion ability is not impaired and the cell number and viability of the final product can fully meet the requirements for clinical treatment. In accordance with the concept that using ribonucleoproteins (RNPs) can reduce the off-target risk[35,36], we have not, indeed, found any indel events using WGS and deep sequencing analyses, thus mitigating the safety concern of genome editing. During the process from bench to production, an unexpected lower CAR recombination efficiency in two infusion products (patient-1, patient-4) and low *PD1* indel percentage in one infusion product (patient-1) were detected. The reason is attributed to the early premature manufacturing process, which has been solved, rather than individual variance or low reproducibility of method. Taken together, we demonstrate the feasibility of formal large-scale production of non-viral genome specific targeted CAR T cells for clinical application.

We are the first to demonstrate the safety and efficacy of non-viral genome

specific targeted CAR T cells in a clinical trial. Relative to conventional CAR T cell therapies[37-39], we found superior safety for patients with r/r B-NHL by using non-viral *PD1*-integrated anti-CD19 CAR T cells, with only a low percentage of mild CRS and without occurrence of neurologic toxicity. Our results are also consistent with two recently reported clinical trials[40,41] and accordingly further demonstrate the safety of CRISPR/Cas9 application in T cell therapy. It was reported that the rates of CR in treating patients with r/r B-NHL by three FDA approved autologous anti-CD19 CAR T cell therapies were 58%[37], 40%[38] and 53%[39], respectively. In contrast, we observed a striking high rate (87.5%) of CR. Surprisingly, despite an unexpectedly low initial dose or simultaneous low CAR percentage, CR was achieved in all three patients, which indicates that non-viral *PD1*-targeted CAR T cells indeed have more potency to kill tumor cells. Thus, it prompts us to test lower infusion doses in future clinical trials, which may further reduce the preparation time and production cost.

The outstanding clinical efficacy can be explained by our scRNA-seq data in two aspects. First, when compared to conventional CAR T cells produced by lentivirus[29], there was a much higher percentage of $CD8^+$ memory cells in the infusion products of non-viral *PD1*-integrated CAR T cells. Second, driven by the loss of PD1, the *in vivo* persistence of fewer dysfunctional CAR T cells was found through the treatment. Additionally, our results revealed that *PD1* knockout causes the downregulation of diverse immune suppressive signaling in CAR T cells, which suggests that gene editing strategy may have an advantage over those that only abolish the interaction between PD1 and PD-L1 by using antibodies. Given that inhibitory receptors which parallel PD1 function, such as LAG3, TIM3 and TIGIT, were still highly expressed in CAR^+ cells according to our data (Figure 4c, S13b, Table S7-S9), simultaneously intervening in multiple pathways holds promise to further augment the function of CAR T cells. In conclusion, our clinical results give solid evidence for the real advantage of non-viral genome specific integrated CAR T cells, thus uncovering its great potential in treating more malignancies, especially solid tumors, in the future.

In this study, we describe an innovative strategy to develop non-viral genome specific targeted CAR T cells by CRISPR/Cas9. This technology is advanced due to

combining the advantages of both non-viral manufacturing processes and precise genome editing. As a two-in-one approach without using virus, the manufacturing procedure is simplified, with shortened preparation time, reduced production expenses, and increased safety and efficacy of CAR T cell products. These advantages are significant, especially for the generation of gene modified CAR T cells where virus preparation and genome editing process are normally both required. On the other hand, locus-specific integration augments the homogeneity of CAR T cells and makes it possible to exploit versatile cell products. Importantly, for the first time, we show the feasible application of this technology from bench to bedside and demonstrate its remarkable safety and efficacy in a clinical trial. Thus, we propose a revolutionary CAR T technology to break through the current barriers and show the considerable potential of CRISPR/Cas9-mediated non-viral genome specific targeted technology in cell therapy.

References

1 Larson, R. C. & Maus, M. V. Recent advances and discoveries in the mechanisms and functions of CAR T cells. *Nat Rev Cancer* **21**, 145-161 (2021).

2 MacKay, M. *et al.* The therapeutic landscape for cells engineered with chimeric antigen receptors. *Nat Biotechnol* **38**, 233-244 (2020).

3 June, C. H., O'Connor, R. S., Kawalekar, O. U., Ghassemi, S. & Milone, M. C. CAR T cell immunotherapy for human cancer. *Science* **359**, 1361-1365 (2018).

4 June, C. H. & Sadelain, M. Chimeric Antigen Receptor Therapy. *N Engl J Med* **379**, 64-73 (2018).

5 Labanieh, L., Majzner, R. G. & Mackall, C. L. Programming CAR-T cells to kill cancer. *Nature Biomedical Engineering* **2**, 377-391 (2018).

6 Michieletto, D., Lusic, M., Marenduzzo, D. & Orlandini, E. Physical principles of retroviral integration in the human genome. *Nat Commun* **10**, 575 (2019).

7 Russo-Carbolante, E. M. D. *et al.* Integration pattern of HIV-1 based lentiviral vector carrying recombinant coagulation factor VIII in Sk-Hep and 293T cells. *Biotechnology Letters* **33**, 23-31 (2011).

8 Atianand, M. K. & Fitzgerald, K. A. Molecular basis of DNA recognition in the immune system. *J Immunol* **190**, 1911-1918 (2013).

9 Tao, J. L., Zhou, X. & Jiang, Z. F. cGAS-cGAMP-STING: The Three Musketeers of Cytosolic DNA Sensing and Signaling. *Iubmb Life* **68**, 858-870 (2016).

10 Gandara, C., Affleck, V. & Stoll, E. A. Manufacture of Third-Generation Lentivirus for Preclinical Use, with Process Development Considerations for Translation to Good Manufacturing Practice. *Human Gene Therapy Methods* **29**, 1-15 (2018).

11 Hurton, L. V. *et al.* Tethered IL-15 augments antitumor activity and promotes a stem-cell memory subset in tumor-specific T cells. *Proceedings of the National Academy of Sciences of the United States of America* **113**, E7788-E7797 (2016).

12 Kebriaei, P. *et al.* Phase I trials using Sleeping Beauty to generate CD19-specific CAR T cells. *Journal of Clinical Investigation* **126**, 3363-3376 (2016).

13 Maiti, S. N. *et al.* Sleeping Beauty System to Redirect T-cell Specificity for Human Applications. *Journal of Immunotherapy* **36**, 112-123 (2013).

14 Monjezi, R. *et al.* Enhanced CAR T-cell engineering using non-viral Sleeping Beauty transposition from minicircle vectors. *Leukemia* **31**, 186-194 (2017).

15 Foster, J. B. *et al.* Purification of mRNA Encoding Chimeric Antigen Receptor Is Critical for Generation of a Robust T-Cell Response. *Human Gene Therapy* **30**, 168-178 (2019).

16 Lin, L. *et al.* Preclinical evaluation of CD8+anti-BCMA mRNA CAR T cells for treatment of multiple myeloma. *Leukemia* (2020).

17 Eyquem, J. *et al.* Targeting a CAR to the TRAC locus with CRISPR/Cas9 enhances tumour rejection. *Nature* **543**, 113-+ (2017).

18 Dai, X. Y. *et al.* One-step generation of modular CAR-T cells with AAV-Cpf1. *Nat Methods* **16**, 247-+ (2019).

19 Roth, T. L. *et al.* Reprogramming human T cell function and specificity with non-viral genome targeting. *Nature* **559**, 405-409 (2018).

20 Cherkassky, L. *et al.* Human CAR T cells with cell-intrinsic PD-1 checkpoint blockade resist tumor-mediated inhibition. *Journal of Clinical Investigation* **126**, 3130-3144 (2016).

21 John, L. B. *et al.* Anti-PD-1 Antibody Therapy Potently Enhances the Eradication of Established Tumors By Gene-Modified T Cells. *Clinical Cancer Research* **19**, 5636-5646 (2013).

22 Rafiq, S. *et al.* Targeted delivery of a PD-1-blocking scFv by CAR-T cells enhances anti-tumor efficacy in vivo. *Nat Biotechnol* **36**, 847-856 (2018).

23 Ren, J. T. *et al.* Multiplex Genome Editing to Generate Universal CAR T Cells Resistant to PD1 Inhibition. *Clinical Cancer Research* **23**, 2255-2266 (2017).

24 Rupp, L. J. *et al.* CRISPR/Cas9-mediated PD-1 disruption enhances anti-tumor efficacy of human chimeric antigen receptor T cells. *Sci Rep* **7**, 737 (2017).

25 Su, S. *et al.* CRISPR-Cas9 mediated efficient PD-1 disruption on human primary T cells from cancer patients. *Sci Rep* **6**, 20070 (2016).

26 Guo, X. *et al.* Disruption of PD-1 Enhanced the Anti-tumor Activity of Chimeric Antigen Receptor T Cells Against Hepatocellular Carcinoma. *Front Pharmacol* **9**, 1118 (2018).

27 van der Leun, A. M., Thommen, D. S. & Schumacher, T. N. CD8(+) T cell states in human cancer: insights from single-cell analysis. *Nature Reviews Cancer* **20**, 218-232 (2020).

28 Sade-Feldman, M. *et al.* Defining T Cell States Associated with Response to Checkpoint Immunotherapy in Melanoma. *Cell* **175**, 998-+ (2018).

29 Deng, Q. *et al.* Characteristics of anti-CD19 CAR T cell infusion products associated with efficacy and toxicity in patients with large B cell lymphomas. *Nat Med* **26** (2020).

30 Thommen, D. S. *et al.* A transcriptionally and functionally distinct PD-1(+) CD8(+) T cell pool with predictive potential in non-small-cell lung cancer treated with PD-1 blockade. *Nat Med* **24**, 994-+ (2018).

31 Zheng, C. H. *et al.* Landscape of Infiltrating T Cells in Liver Cancer Revealed by Single-Cell Sequencing. *Cell* **169**, 1342-+ (2017).

32 Doudna, J. A. The promise and challenge of therapeutic genome editing. *Nature* **578**, 229-236 (2020).
33 Hsu, P. D., Lander, E. S. & Zhang, F. Development and Applications of CRISPR-Cas9 for Genome Engineering. *Cell* **157**, 1262-1278 (2014).
34 Komor, A. C., Badran, A. H. & Liu, D. R. CRISPR-Based Technologies for the Manipulation of Eukaryotic Genomes. *Cell* **168**, 20-36 (2017).
35 Liang, X. Q. *et al.* Rapid and highly efficient mammalian cell engineering via Cas9 protein transfection. *J Biotechnol* **208**, 44-53 (2015).
36 Kim, S., Kim, D., Cho, S. W., Kim, J. & Kim, J. S. Highly efficient RNA-guided genome editing in human cells via delivery of purified Cas9 ribonucleoproteins. *Genome Res* **24**, 1012-1019 (2014).
37 Locke, F. L. *et al.* Long-term safety and activity of axicabtagene ciloleucel in refractory large B-cell lymphoma (ZUMA-1): a single-arm, multicentre, phase 1-2 trial. *Lancet Oncol* **20**, 31-42 (2019).
38 Schuster, S. J. *et al.* Tisagenlecleucel in Adult Relapsed or Refractory Diffuse Large B-Cell Lymphoma. *N Engl J Med* **380**, 45-56 (2019).
39 Abramson, J. S. *et al.* Lisocabtagene maraleucel for patients with relapsed or refractory large B-cell lymphomas (TRANSCEND NHL 001): a multicentre seamless design study. *Lancet* **396**, 839-852 (2020).
40 Lu, Y. *et al.* Safety and feasibility of CRISPR-edited T cells in patients with refractory non-small-cell lung cancer. *Nat Med* **26**, 732-740 (2020).
41 Stadtmauer, E. A. *et al.* CRISPR-engineered T cells in patients with refractory cancer. *Science* **367**, 1001-+ (2020).
42 Lee, D. W. *et al.* Current concepts in the diagnosis and management of cytokine release syndrome. *Blood* **124**, 188-195 (2014).
43 Liu, Q. *et al.* Hi-TOM: a platform for high-throughput tracking of mutations induced by CRISPR/Cas systems. *Sci China Life Sci* **62**, 1-7 (2019).
44 Li, H. & Durbin, R. Fast and accurate short read alignment with Burrows-Wheeler transform. *Bioinformatics* **25**, 1754-1760 (2009).
45 Li, H. *et al.* The Sequence Alignment/Map format and SAMtools. *Bioinformatics* **25**, 2078-2079 (2009).
46 Chen, S. F., Zhou, Y. Q., Chen, Y. R. & Gu, J. fastp: an ultra-fast all-in-one FASTQ preprocessor. *Bioinformatics* **34**, 884-890 (2018).
47 Yaari, G., Bolen, C. R., Thakar, J. & Kleinstein, S. H. Quantitative set analysis for gene expression: a method to quantify gene set differential expression including gene-gene correlations. *Nucleic Acids Res* **41** (2013).
48 Hanzelmann, S., Castelo, R. & Guinney, J. GSVA: gene set variation analysis for microarray and RNA-Seq data. *Bmc Bioinformatics* **14** (2013).

Methods

Clinical trial information and design

This study was a phase I, single-arm clinical trial designed to evaluate the

safety and efficacy of non-viral *PD1*-integrated anti-CD19 CAR T cells in treating relapsed/refractory (r/r) aggressive B-cell non-Hodgkin lymphoma (B-NHL). The clinical protocol has been registered at ClinicalTrials.gov (NCT04213469). The inclusion criteria were as follows: 1) aged 18 to 70 years old; 2) diagnosed with CD19 positive r/r B-NHL (stage III-IV); 3) life expectancy of >3 months; 4) with Eastern Cooperative Oncology Group (ECOG) score of ≤2 and satisfactory major organ functions; 5) a negative pregnancy test for women of reproductive potential and agreement of using birth control during the study. The exclusion criteria included: 1) pregnancy or breast feeding women; 2) refusal to use birth control during the next two years; 3) underwent allo-HSCT within six months or previous treatment of graft versus host disease; 4) active autoimmune disease which requires immunosuppressive agents; 5) active infection; 6) history of other malignances; 7) ineligibility or lack of ability to comply with the study. In order to preliminarily assess the safety and effectiveness of this novel CAR T cell therapy, eight patients were enrolled in the cohort with infusion dose of 2×10^6 CAR T cells/kg. Due to the premature manufacturing process and individual variance, the cell number of three infusion products could not meet the planned dose requirement, thus the actual infusion doses in these patients were lower than 1×10^6/kg (Table 1, S3). This therapy included 3 days of lymphodepletion chemotherapy using combined fludarabine (25 mg/m2 from day -4 to -2) and cyclophosphamide (250 mg/m2 from day -3 to -2). CAR T cell infusion was performed 2 days after the end of lymphodepletion chemotherapy and was followed by standard monitoring. All patients provided written informed consent in accordance with the Declaration of Helsinki before enrolment in the study. The clinical protocol was reviewed and approved by the Clinical Research Ethics Committee of the First Affiliated Hospital, College of Medicine, Zhejiang University. Characteristics, clinical responses and prior therapies of the patients are shown in Table 1 and Table S4. Non-viral *PD1*-targeted CAR T cells for clinical treatment were manufactured by Bioray Laboratories Inc.

Response assessment

Treatment response was assessed according to a revised criteria of the Lugano classification. PET-CT scans and bone marrow biopsy were the major methods applied to evaluate the lymphoma lesions. The response assessment criteria were as follows: 1) CR (complete remission): absence of clinical symptoms, PET-CT and bone marrow evidence associated with lymphoma; 2) PR (partial remission): lymphoma volume decreases at least 50% without new lymphoma lesions or sustained bone marrow involvement; 3）PD (progressive disease): lymphoma volume increases at least 50% or onset of new lymphoma lesions; 4) SD (stable disease): a condition achieving the criteria for none of CR, PR or PD. The response duration was calculated from the first documentation of response, until progression, initiation of off-study treatment or the last documentation of ongoing response.

Assessment and grading of cytokine release syndrome

Serum cytokines including IL-2, IL-4, IL-6, IL-10, IFN-γ, TNF-α and IL-17A were assessed by Human Th1/Th2/Th17 CBA Kit (BD Biosciences) within one month after infusion. Cytokine release syndrome (CRS) was assessed and graded according to the National Cancer Institute Common Terminology Criteria for Adverse Events (NCI-CTCAE) version 5.0 in combination with other methods[42].

Assessment and grading of neurological toxicity

Neurological toxicities were assessed and graded according to CTCAE version 5.0. Once CRS symptoms such as pyrexia, hypotension and capillary leak, or other types of adverse events (AEs) were observed, the patient would be closely monitored for signs of neurological toxicity, such as seizure, tremor, encephalopathy and dysphasia.

Assessment and grading of adverse events

Patients were inpatients and closely monitored after receiving lymphodepletion chemotherapy and CAR T cell infusion. Physical and clinical laboratory examinations were documented during hospitalization to evaluate the toxicity of the treatment. AEs were graded using CTCAE version 5.0. All AEs are summarized in Table S5. During

hospitalization, any AEs that occurred after CAR T cell infusion were recorded. Severe AEs, except the decrease of lymphocyte counts caused by lymphodepletion chemotherapy, were required to be reported to the Medical Ethics Committee of the First Affiliated Hospital, College of Medicine, Zhejiang University within 24 hours of the occurrence. One month after infusion, patients were followed up and monitored for disease progression and toxicity once a month.

Cell lines

Nalm-6 and Raji cells were purchased from ATCC and maintained in RPMI1640 medium (ThermoFisher) supplemented with 10% fetal bovine serum (ThermoFisher). A Raji cell line stably expressing firefly luciferase (ffLuc) was established by lentivirus infection. Raji cells stably expressing PD-L1 were generated using a lentivirus vector containing a co-expression cassette for PD-L1 and ffLuc. All the stable cell lines underwent selection with puromycine.

Isolation and expansion of human primary T cells

Fresh peripheral blood mononuclear cells (PBMCs) from healthy donors were provided by Shanghai SAILY Biological Technology Co., Ltd. Fresh PBMCs from patients were collected by apheresis. PBMCs were isolated by density gradient centrifugation using Ficoll (Sigma-Aldrich). T cells were enriched via magnetic separation using anti-CD8/CD4 microbeads (Miltenyi Biotech) and activated with T Cell TransAct (Miltenyi Biotech). T cells were cultured in X-VIVO media (Lonza) supplemented with 2% human AB serum or CTS™ Immune Cell Serum Replacement (ThermoFisher) and recombinant human IL-2 (100 units/mL), IL-7 (5 ng/mL) and IL-15 (5 ng/mL). Cells were harvested once the number reached the requirement for administration, and then washed, formulated and cryopreserved.

CAR T cell generation by lentivirus

The Anti-CD19 CAR cassette was composed of humanized single-chain variable fragment (scFv) derived from clone FMC63, the extracellular domain and

transmembrane regions of CD8α, the intracellular domain of 4-1BB (CD137), and the intracellular domain of CD3ζ. The CAR sequence was cloned into the pCDH lentiviral vector backbone containing an EF1α promoter. Lentiviruses were produced by transfecting 293T cells with CAR plasmid, pMD2.G and psPAX2 using polyethylenimine (PEI). Virus supernatants were harvested after 3 days to infect primary human T cells.

RNP and linear double-stranded DNA production

One two-component single guide RNA (sgRNA) targeting *AAVS1* (5'-AGAGCUAGCACAGACUAGAG-3') or *PD1* (5'-CGACUGGCCAGGGCGCCUGU-3') was chemically synthesized (GenScript) and resuspended with TE buffer. Ribonucleoproteins (RNPs) were produced by complexing AAVS1 or PD1 sgRNA and recombinant spCas9 (ThermoFisher) for 10 minutes at room temperature. RNPs were subjected to electroporation immediately after complex formation. For linear double-stranded DNA (dsDNA) production in preclinical experiments, plasmids containing an mTurquoise2 or anti-CD19 CAR sequence flanked by homology arms were first constructed. The linear dsDNA was then obtained by restriction endonuclease digestion and purified by TIANgel DNA Purification Kit (Tiangen Biotech).

Human primary T cell electroporation

Electroporation was performed 2-3 days after T cell stimulation. The procedure was conducted following the manufacturer's instructions using a Lonza 4D electroporation system. Briefly, pre-washed T cells were resuspended in the electroporation buffer P3. Meanwhile, RNPs were prepared followed by mixture with the DNA template. Cells in electroporation buffer were then added and moved into electroporation cuvettes. The program of EO115 was chosen for electroporation. After electroporation, pre-warmed media was immediately supplemented and cells were transferred away from electroporation cuvettes.

Indel percentage analysis

Genomic DNA was obtained using a Genomic DNA Purification Kit (ThermoFisher). The fragments containing indel sites were amplified by PCR using specific primers and purified by TIANgel DNA Purification Kit (Tiangen Biotech). DNA sequencing was carried out and indel percentage was measured by ICE analysis (Synthego). The primers used were as follows: AAVS1-Forward 5'-CACCACGTGATGTCCTCTGA-3'; AAVS1-Reverse 5'-CCGGCCCTGGGAATATAAGG-3'; PD1-Forward 5'-CCACGTGGATGTGGAGGAAG-3'; PD1-Reverse: 5'-CCACACAGCTCAGGGTAAGG-3'.

Deep Sequencing

Deep sequencing was carried out to detect indels at 29 top-ranked off-target sites predicted by the Benchling CRISPR tool or to validate the possible indels preliminarily indicated by whole genome sequencing in one representative infusion product (patient-2). Genomic DNA of untreated T cells and infusion products was harvested using Genomic DNA Purification Kit (ThermoFisher). The fragments containing indel sites were amplified by PCR using specific primers and subjected to sequencing on a Hi-TOM platform with 10000× coverage as described previously[43].

Whole Genome Sequencing

Genomic DNA of untreated T cells and the infusion product of patient-2 was extracted using Blood & Cell Culture DNA Kit (Qiagen) according to the manufacturer's instructions and subjected to library construction. Sequencing libraries were generated using Truseq Nano DNA HT Sample preparation Kit (Illumina) following the manufacturer's recommendations and index codes were added to attribute sequences to each sample. These libraries including untreated and edited T cells were sequenced on the HiSeq platform (Illumina) with 100× coverage. BWA (Burrows-Wheeler Aligner)[44] was used to align the clean reads of each sample against the reference genome (settings: mem -t 5 -M -R). Alignment files were converted to

BAM files using SAMtools software[45] (settings: -bS -t). In addition, potential PCR duplications were removed using the sambamba command "markdup". If multiple read pairs have identical external coordinates, only the pair with the highest mapping quality was retained. Insertions and deletions (indels) (<50bp) were calculated and identified with MPILEUP in SAMTOOLS[45]. In order to reduce the indel detection error rate, we filtered the indels in which the supported reads number was less than 4 and quality value (MQ) was less than 30 and QUAL was less than 20. Indels were filtered, with those near other variants and within the PAR being removed. The whole genome sequencing was carried out by Novogene Co., Ltd.

We used Cas-OFFinder (http://www.rgenome.net/cas-offinder/) to predict potential off-target sites. Any sequence, followed by an NRG PAM, having no more than five mismatches (a bulge penalty equals two base mismatches) with PD1 sgRNA, was screened and in total 2,219 sites (not including those around on-target site) were identified. Indels exclusively detected in the edited sample and located around potential off-target sites were searched. No indel events were found within 15bp upstream and downstream (±15bp) of the sites. Indel events were detected within 200bp upstream and downstream (±200bp) of 8 sites. Deep sequencing with 10000 × coverage was performed to validate these indel events.

Single-cell RNA sequencing

Fresh PBMCs from patients were collected by apheresis at the peak (D7 or D12) and stable (D28 or D29) stages of CAR T cell expansion after infusion, respectively, and then isolated by density gradient centrifugation using Ficoll (Sigma-Aldrich). Infusion products and PBMCs of three patients (patient-1, patient-2, patient-3) were subjected to single-cell RNA sequencing (scRNA-seq).

The scRNA-seq libraries were generated using the 10X Genomics Chromium Controller Instrument and Chromium Single Cell 3' V3.1 Reagent Kits (10× Genomics). Briefly, cells were concentrated to 1000 cells/μL and approximately 7,000 cells were loaded into each channel to generate single-cell Gel Bead-In-Emulsions (GEMs), which results in mRNA barcoding of an expected 5,000 single-cells for each sample. After the RT step, GEMs were broken and barcoded-cDNA was purified and amplified. The amplified barcoded cDNA was fragmented, A-tailed, ligated with adaptors and index PCR amplified. The final libraries were quantified using the Qubit

High Sensitivity DNA assay (ThermoFisher) and the size distribution of the libraries was determined using a High Sensitivity DNA chip on a Bioanalyzer 2200 (Agilent). All libraries were sequenced by an Illumina sequencer (Illumina) on a 150bp paired-end run.

We applied fastp[46] with default parameter filtering of the adaptor sequence and removed the low quality reads to achieve clean data. Then the feature-barcode matrices were obtained by aligning reads to the human genome (GRCh38 Ensemble: version 91) using CellRanger v3.1.0. We applied the down sample analysis among samples sequenced according to the mapped barcoded reads per cell of each sample and finally achieved the aggregated matrix. Cells containing over 200 expressed genes and a mitochondria UMI rate below 20% passed the cell quality filtering and mitochondrial genes were removed in the expression table.

Seurat package (version: 3.1.4, https://satijalab.org/seurat/) was used for cell normalization and regression based on the expression table according to the UMI counts of each sample and percent of mitochondria rate to obtain the scaled data. PCA was performed based on the scaled data with the top 2000 highly variable genes and the top 10 principals used for tSNE construction and UMAP construction. Utilizing the graph-based cluster method, we acquired the unsupervised cell cluster result based the PCA top 10 principals and we calculated the marker genes by the FindAllMarkers function with the Wilcox rank sum test algorithm under the following criteria: 1) lnFC >0.25; 2) pvalue <0.05; 3) min.pct >0.1. To characterize the relative activation of a given gene set such as KEGG pathway, Memory, Dysfunction and Cytotoxicity as described previously, we used QuSAGE[47] (2.16.1) to calculate the score for each cluster/sample and GSVA[48] (1.32.0) to calculate it for each cell. ScRNA-seq and data analysis were performed by NovelBio Bio-Pharm Technology Co., Ltd.

Flow cytometry

CAR and membrane protein expression was determined by flow cytometry. Cells were pre-washed and incubated with antibodies for 30 minutes on ice. After washing twice, samples were run on an LSRFortessa (BD Biosciences) and analyzed with FlowJo software. The following antibodies were used: FITC anti-human CD3, APC anti-human CD69, APC anti-human CD137, APC anti-human CD25, APC anti-human PD1, APC anti-human LAG3, BV421 anti-human CD45RO, APC

anti-human CD62L, APC anti-human CD3, FITC anti-human CD19, FITC anti-human CD4, APC anti-human CD4, APC anti-human CD8 (All from BioLegend), PerCP-Cy™5.5 anti-human CD45 (BD Biosciences). For detection of CAR expression, biotinylated human CD19 (aa 20-291) protein (ACRO Biosystems) and PE Streptavidin (BioLegend) were added in order, or PE-labeled human CD19 (aa 20-291) protein (ACRO Biosystems) was used. For some experiments, CAR T cells were co-cultured with target cells at an E/T 1:1 (AAVS1-19bbz experiments) or 1:2 (PD1-19bbz experiments) ratio for 24 hours before harvest. For detection of clinical samples, peripheral blood cells were stained with antibodies, followed by addition of Lysing Buffer (BD Biosciences) before running. CAR percentage was analyzed in $CD45^+/CD3^+$ gated cells.

CAR copy number analysis by qPCR

Blood samples were collected before and after CAR T cell infusion. Lysis Buffer (BD Biosciences) was first added and genomic DNA was acquired using Genomic DNA Purification Kit (ThermoFisher). A seven-point standard curve was generated by using 5×10^0-5×10^6 copies/μL lentiviral vector DNA containing the 19bbz sequence. TaqMan qPCR assay was performed to measure CAR copy number in peripheral blood cells. qPCR was run on a QuantStudio™ 3 Real-Time PCR System (ThermoFisher). Each sample was determined in triplicate. Primers specifically targeting the 19bbz sequence were as follows: Forward 5'-GCTGTAGCTGCCGATTTCCA-3', Reverse 5'-GGTTCTGGCCCTGCTTGTAC-3', Probe 5'-AGTGAAGTTCAGCAGGAGCGCAGACG-3'.

Antigen stimulation and proliferation of CAR T cells

As antigen for stimulation, Raji or PD-L1 expressing Raji cells were pre-treated with mitomycin C (50 μg/ml) for 90 minutes at 37℃. CAR T cells were co-cultured with target cells at an E/T 1:1 (AAVS1-19bbz experiments) or 1:2 (PD1-19bbz experiments) ratio for 3-4 days per stimulation. The number of CAR^+ cells was

enumerated by multiplying the total cell number and the CAR percentage. Cell viability was measured by Trypan blue staining.

Cell Trace Violet proliferation assay

AAVS1-19bbz cells were labeled with Cell Trace Violet (ThermoFisher) according to the manufacturer's instructions. Raji cells were pre-treated with mitomycin C (50 μg/ml) for 90 minutes at 37℃. CAR T cells and target cells were mixed at an E/T 1:1 ratio. After 5 days, cells were harvested and run on an LSRFortessa (BD Biosciences).

Bead-based immunoassay

In preclinical experiments, CAR T cells were co-cultured with Raji or PD-L1 expressing Raji cells at an E/T 1:1 (AAVS1-19bbz experiments) or 1:2 (PD1-19bbz experiments) ratio in media without exogenous cytokines. The supernatant was collected after 24 hours and cytokines were measured using LEGENDplex™ bead-based immunoassays (BioLegend) according to the manufacturer's instructions.

ELISA

For *in vitro* evaluation of infusion products, CAR T cells were co-cultured with Nalm-6 cells at an E/T 1:1 ratio in media without exogenous cytokines. The supernatant was collected after 18-24 hours and IFN-γ secretion was measured using Human IFN-gamma ELISA Kit (StemCell) according to the manufacturer's instructions.

Flow cytometry based cytotoxicity assay

AAVS1-19bbz cells were co-cultured with Raji cells at an E/T 1:1 ratio for 18 hours. Flow cytometry was used to determine residual tumor cells by staining with APC anti-human CD3 and FITC anti-human CD19 antibodies. Cells were enumerated using CountBright™ Absolute Counting Beads (ThermoFisher) following the manufacturer's instructions.

642

643 **LDH cytotoxicity assay**

644 CAR T cells were co-cultured with Nalm-6, Raji or PD-L1 expressing Raji cells
645 at indicated E/T ratios. Cytotoxicity was measured by release of lactate
646 dehydrogenase (LDH) using CytoTox 96® Non-Radioactive Cytotoxicity Assay
647 (Promega) according to the manufacturer's instructions.

648

649 ***In vivo* mouse experiments**

650 All animal experiments conformed to the regulations drafted by the Association
651 for Assessment and Accreditation of Laboratory Animal Care in Shanghai and were
652 approved by the East China Normal University Center for Animal Research. For
653 experiments involving AAVS1-19bbz , 6- to 8-week-old NSG male mice were
654 injected intravenously with 2×10^5 ffLuc-transduced Raji cells. 2×10^6 CAR T cells
655 were administered intravenously after 5 days. For experiments using PD1-19bbz, 6-
656 to 8-week-old NSG male mice were inoculated intravenously with 5×10^5
657 ffLuc-transduced PD-L1 expressing Raji cells. 5×10^6 CAR T cells were injected
658 intravenously after 10 days. Bioluminescence images were acquired and analyzed
659 using IVIS Imaging System and software (PerkinElmer).

660

661 **Statistics**

662 Experimental data are presented as mean ± SD or mean ± SEM as
663 described in the figure legends. Data were analyzed by one-way ANOVA or two-way
664 ANOVA as indicated using GraphPad software. A p value <0.05 was considered
665 statistically significant. Asterisks used to indicate significance correspond to ***p
666 <0.001, **p <0.01, *p <0.05. NS, nonsignificance.

667

668

669 **Acknowledgements**

670 We thank Stefan Siwko for discussing and revising this manuscript. This study was
671 supported by National Key R&D Program of China (2019YFA0802802,

2018YFA0507001), National Natural Science Foundation of China (81772622, 91857116, 31871453, 81730008, 81770201), Innovation Program of Shanghai Municipal Education Commission (2017-01-07-00-05-E00011), Key Project of Science and Technology Department of Zhejiang Province (2019C03016) and Natural Science Foundation of Shanghai (18ZR1412300).

Author contributions

J.Z., Y.H., B.D., M.L. and H.H. designed the overall study and wrote the manuscript. Y.H., W.L. and H.H. designed the clinical trial. J.Z., J.Y., Y.T., L.Z. and Y.Q. performed the experiments. J.Z., B.T., Q.T. and Q.W. were responsible for manufacturing and quality control of CAR T cells. Y.H., M.Z., G.W., K.Z., J.C. and Y.L. performed the clinical trial. J.Z., Y.H. and W.L. analyzed the data. Y.W. and D.L. discussed the results and manuscript. B.D., M.L. and H.H. supervised the study. All authors approved the article for submission and publication.

Competing interests

This study was partially supported by Bioray Laboratories Inc. Patents related to this manuscript have been applied.

Figure 1

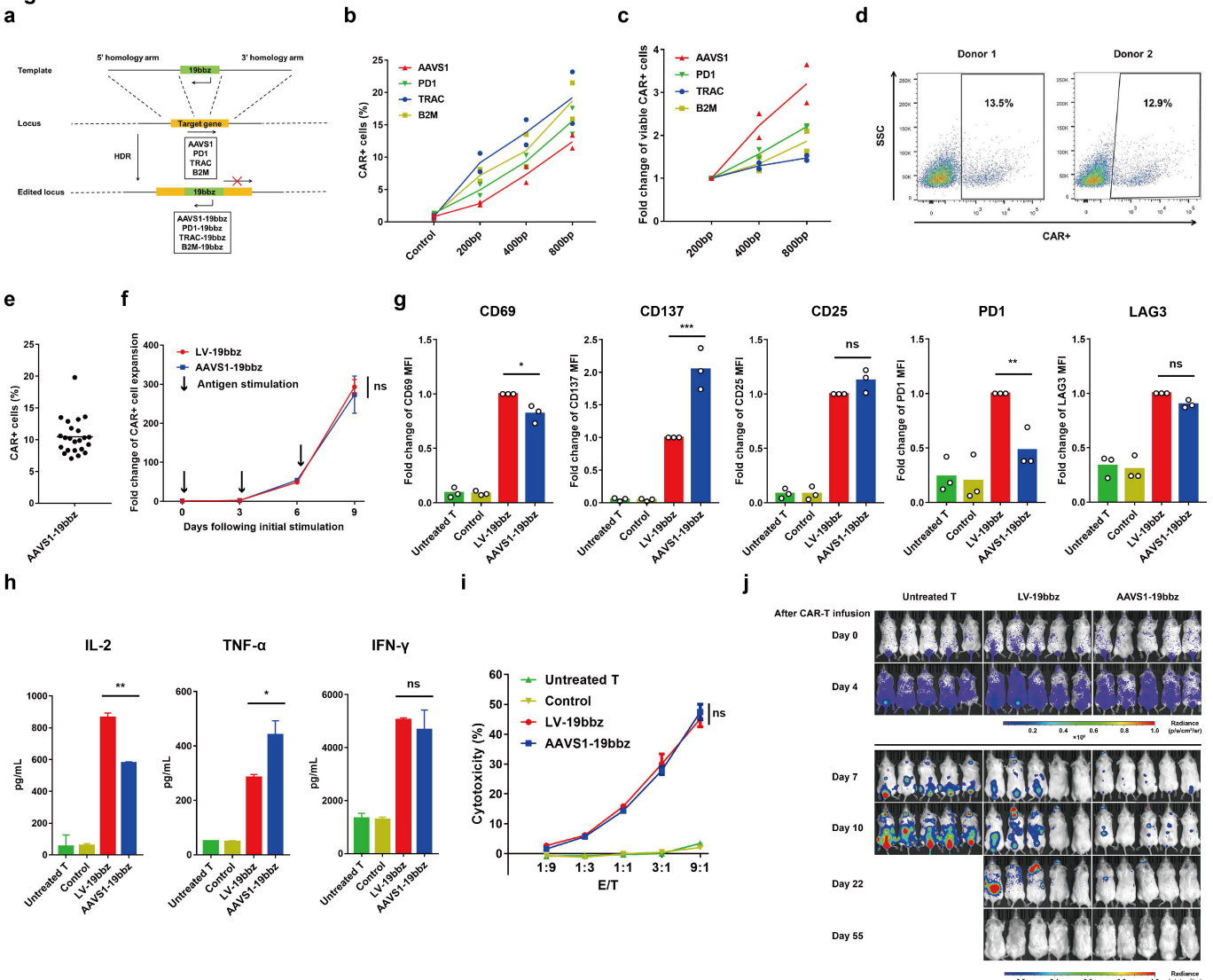

Figure 1 Non-viral *AAVS1*-integrated CAR T cells eliminate tumor cells as effectively as conventional CAR T cells

a, Specific integration of CAR cassette into target locus by homologous recombination through CRISPR/Cas9. HDR, homology directed repair. b-c, Percentage of CAR+ cells (b) and number of viable CAR expressing cells (c) detected 7 days after electroporation using equal mole DNA templates with different homology arm lengths. (n=2 independent healthy donors). d, CAR expression in cells from two representative healthy donors determined 7 days after electroporation. e, Percentage of CAR+ cells detected 7 days after electroporation (n=23 independent healthy donors). f, Expansion of CAR+ cells after repeated stimulation with Raji cells. Data are mean ± SD (n=3 technical replicates). g, Median fluorescent intensity (MFI) of CD69, CD137, CD25, PD1 and LAG3 expression in T cells detected by flow cytometry after 24 hours co-culture with Raji cells (n=3 independent healthy donors). CD3+ (Untreated T, Control) or CD3+/CAR+ (LV-19bbz, AAVS1-19bbz) gated cells were analyzed. h, Representative result of cytokine secretion, measured by bead-based immunoassay, in the supernatant after co-culture with Raji cells for 24 hours. Data are mean ± SD (n=2 technical replicates). i, *In vitro* cytotoxicity against Raji cells as determined by LDH assay. E/T, effector/target. Data are mean ±SD (n=3 technical replicates). j, Bioluminescence imaging of Raji tumor cell growth in NSG mice following different treatments (n=5). Control samples were electroporated the same as AAVS1-19bbz cells except without sgRNA addition. Mean value is shown in b, c, e, g. P values are calculated by one-way ANOVA (g, h) or two-way ANOVA (f, i).

Figure 2

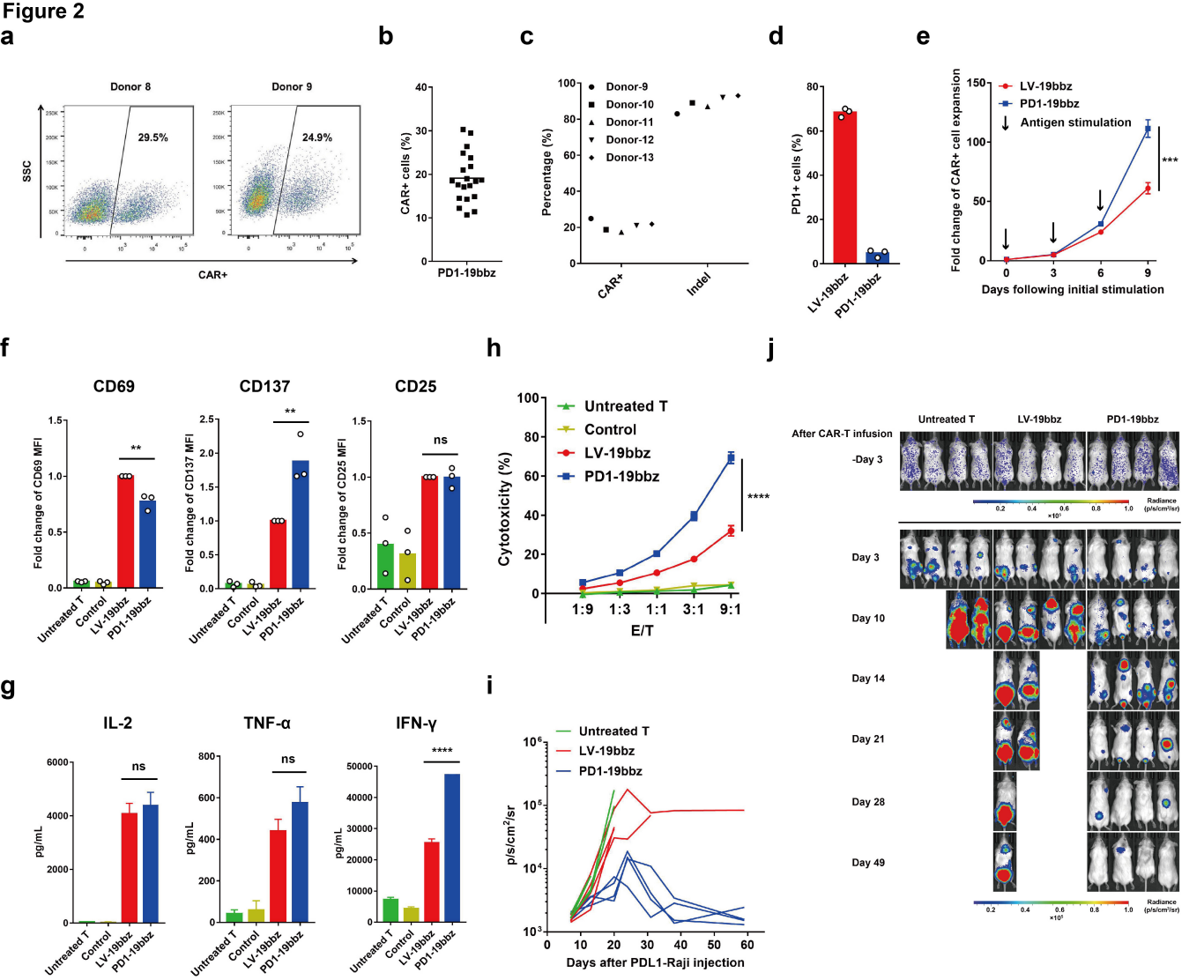

Figure 2 Non-viral *PD1*-integrated CAR T cells outperform conventional CAR T cells

a, CAR expression determined 7 days after electroporation of cells from two representative healthy donors. b, Percentage of CAR+ cells detected 7 days after electroporation (n=20 independent healthy donors). c, Percentages of CAR integration and *PD1* indels in total T cells were detected 7 days after electroporation in five representative healthy donors. d, Percentage of PD1 expression detected by flow cytometry in CD3+/CAR+ gated cells after 24 hours co-culture with PD-L1 expressing Raji cells (n=3 independent healthy donors). e, Expansion of CAR+ cells after repeated stimulation with PD-L1 expressing Raji cells. Data are mean ± SD (n=3 technical replicates). f, MFI of CD69, CD137 and CD25 expression in T cells detected by flow cytometry after 24 hours co-culture with PD-L1 expressing Raji cells (n=3 independent healthy donors). CD3+ (Untreated T, Control) or CD3+/CAR+ (LV-19bbz, PD1-19bbz) gated cells were analyzed. g, Representative result of cytokine secretion in the supernatant (measured by bead-based immunoassay) after co-culture with PD-L1 expressing Raji cells for 24 hours. Data are mean ± SD (n=2 technical replicates). h, *In vitro* cytotoxicity against PD-L1 expressing Raji cells determined by LDH assay. Data are mean ± SD (n=3 technical replicates). i-j, Bioluminescence kinetics (i) and imaging (j) of PD-L1 expressing Raji tumor cell growth in NSG mice following different treatments (n=4). Control samples were electroporated the same as PD1-19bbz cells except without sgRNA addition. Mean value is shown in b, d, f. P values are calculated by one-way ANOVA (f, g) or two-way ANOVA (e, h).

Figure 3

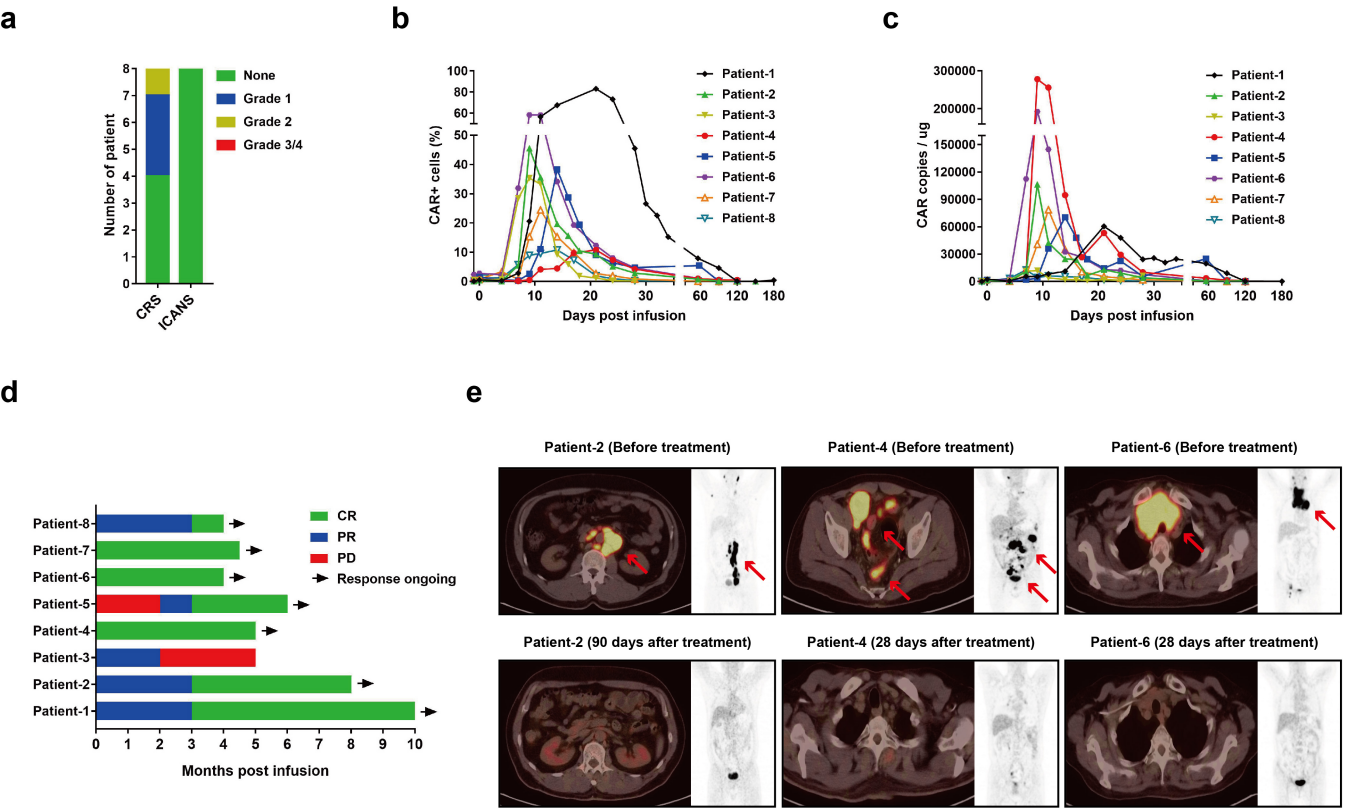

Figure 3 Non-viral *PD1*-integrated CAR T cells potently eliminate tumor cells in patients with r/r B-NHL without serious toxicity

a, Percentages of CRS and ICANS occurrence after treatment. CRS, cytokine release syndrome. ICANS, immune effector cell-associated neurotoxicity syndrome. b, Percentage of CAR+ cells in the peripheral blood T cells of patients on indicated days before and after infusion. c, CAR copy number in genomic DNA from the peripheral blood of patients is shown on indicated days before and after infusion. d, Treatment responses and duration of responses after infusion. CR, complete remission. PR, partial remission. PD, progressive disease. e, PET-CT scans for three representative patients before and after treatment. Red arrows indicate the tumor lesions.

Figure 4

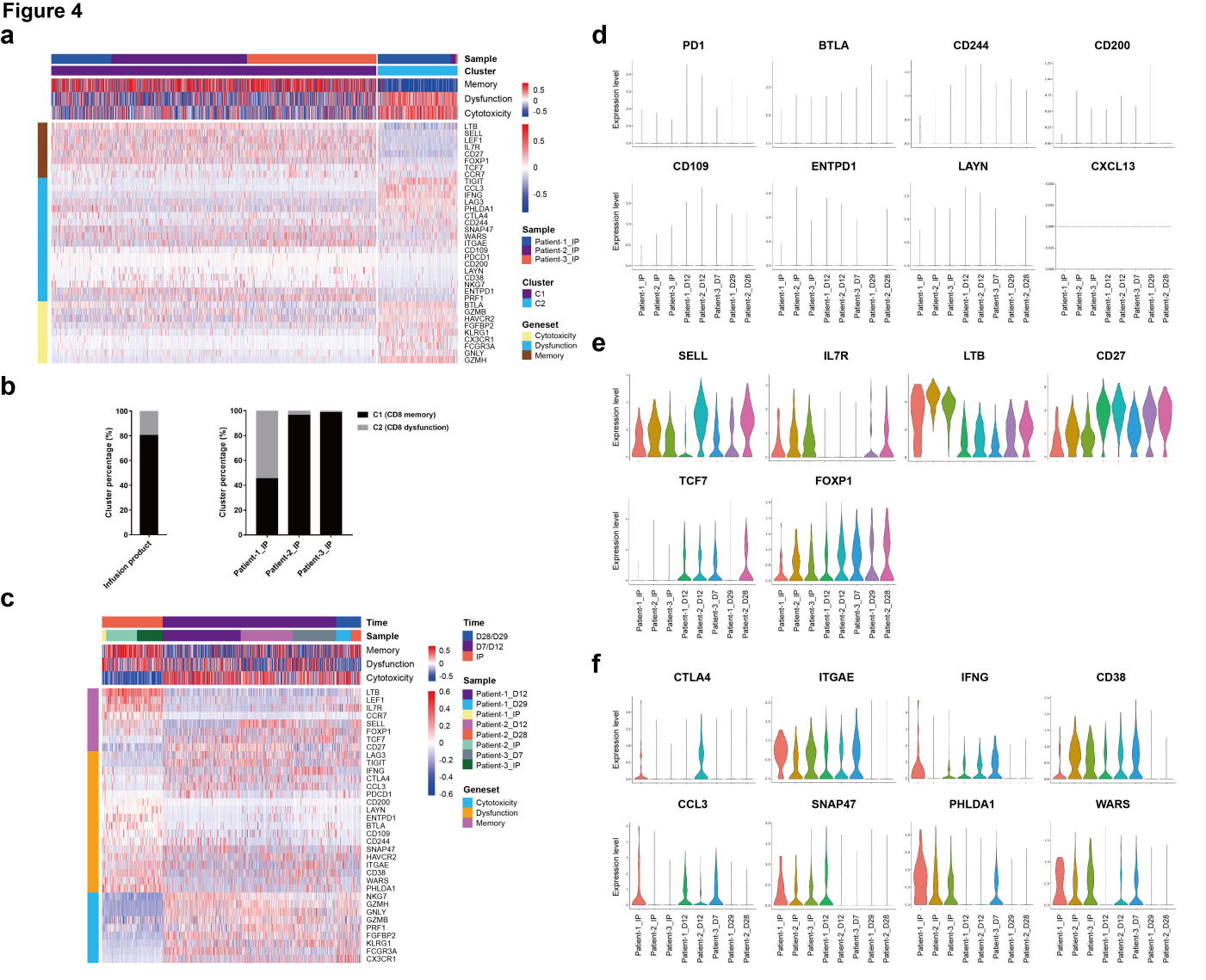

Figure 4 Single-cell RNA sequencing of non-viral *PD1*-integrated CAR T cells before and after infusion

a, Heat map showing scaled expression of memory, dysfunction and cytotoxicity genes in two CD8+ T cell clusters in three infusion products (IP). The scGSVA scores of CD8 memory, dysfunction and cytotoxicity signatures are shown at the top. Cluster 1 (C1) and cluster 2 (C2) were generated by clustering CD8 memory and dysfunction marker genes, respectively. b, Percentages of C1 and C2 in mixed and individual samples of infusion products. c, Heat map showing scaled expression of memory, dysfunction and cytotoxicity genes in CD8+/CAR+ cells from three patients before and after infusion. The scGSVA scores of CD8 memory, dysfunction and cytotoxicity signatures are shown at the top. d-f, Violin plots showing the expression of PD1 (d), PD1-associated inhibitory genes (d), memory genes (e) and dysfunction genes (f) in CD8+/CAR+ cells from three patients before and after infusion. The data of patient-3 sample after 28 days treatment is not shown due to an unreliable low CAR+ cell number.

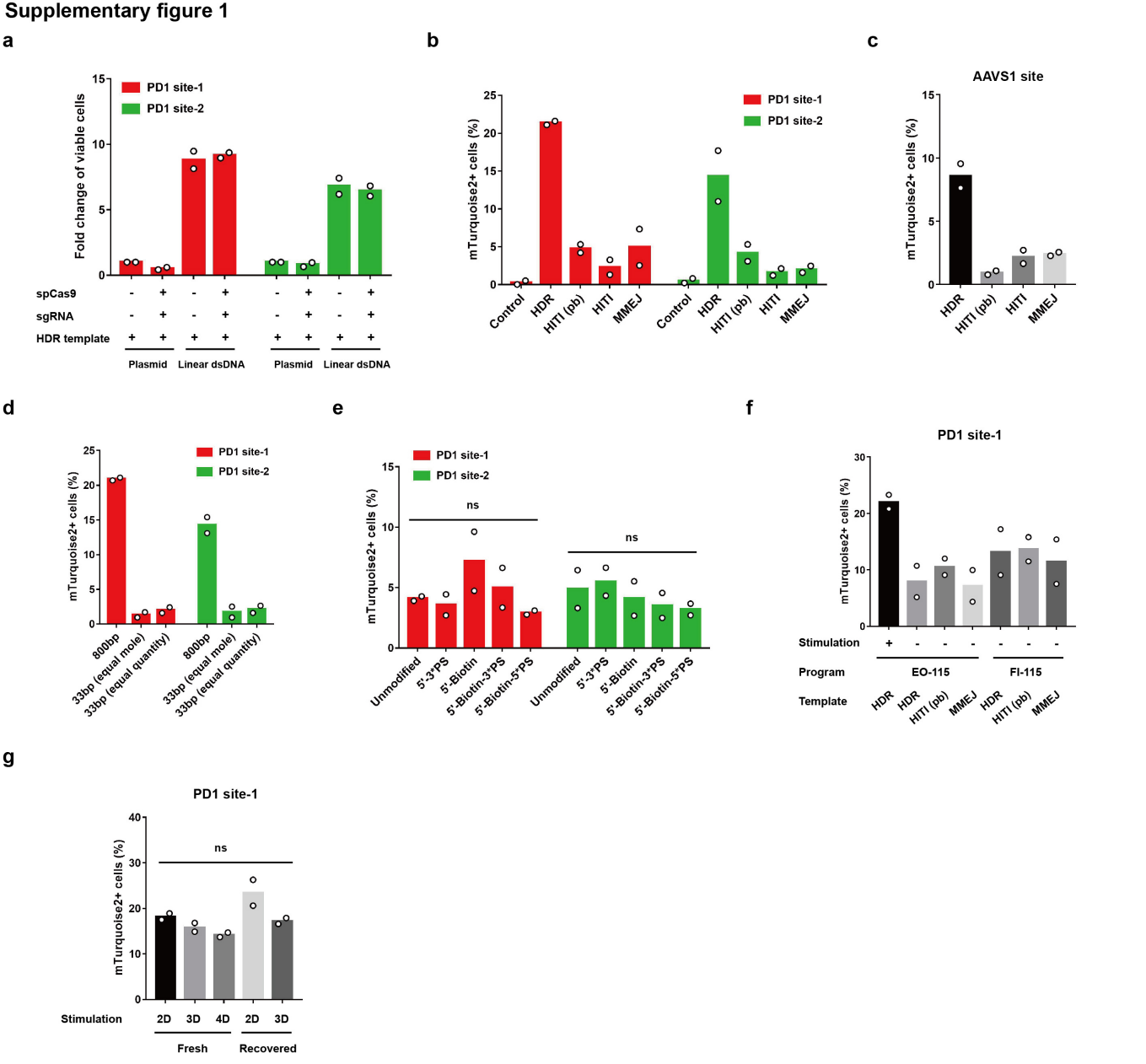

Supplementary figure 1 Optimization of the conditions for constructing non-viral genome specific targeted T cells

The sequence of fluorescent protein mTurquoise2 was used as a target to optimize the conditions for generating non-viral genome specific integrated T cells. a, Number of viable cells calculated 7 days after electroporation by using different protocols. Equal quantities of circular plasmid DNA and linear double-stranded DNA (dsDNA) were used. Due to acquisition of higher cell viability, templates in the form of linear dsDNA were chosen for all the following experiments. b-c, Recombination efficiency of mTurquoise2 at two *PD1* sites (b) and one *AAVS1* site (c) by using different DNA templates. HDR, homology directed repair. HITI, homology-independent targeted integration. HITI (pb), HITI template with 50bp protection base pairs flanking the target sequence. MMEJ, microhomology-mediated end joining. d, Recombination efficiency of mTurquoise2 using 33bp or 800bp homology arms. Equal mole or quantity of template harboring 33bp homology arms was used, compared with template with 800bp homology arms. e, Recombination efficiency of mTurquoise2 by using unmodified or modified DNA templates with 200bp homology arms. PS, phosphorothioate. Biotin was modified at the first base pair from the 5' side. PS was modified at the first three or five base pairs from the 5' side. f, Recombination efficiency of mTurquoise2 in unstimulated or stimulated T cells using different programs and DNA templates. g, Recombination efficiency of mTurquoise2 in fresh or recovered T cells after stimulation for indicated days by using HDR templates with 800bp homology arms. 800bp and 20bp homology arms were used in HDR and MMEJ templates, respectively. Equal moles of DNA template were used in b, c, e-g. The recombination efficiency was determined 7 days after electroporation in b-g. All the experiments were performed in cells from two independent healthy donors. Mean value is shown in all the figures. P values are calculated by one-way ANOVA (g) or two-way ANOVA (e).

Supplementary figure 2

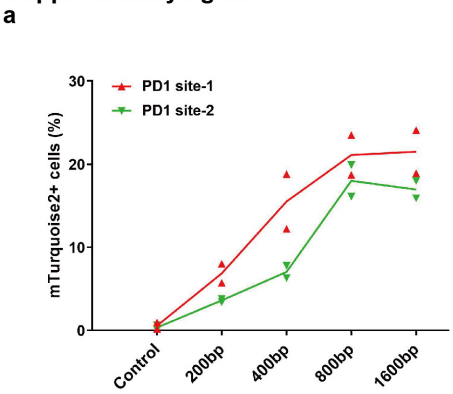

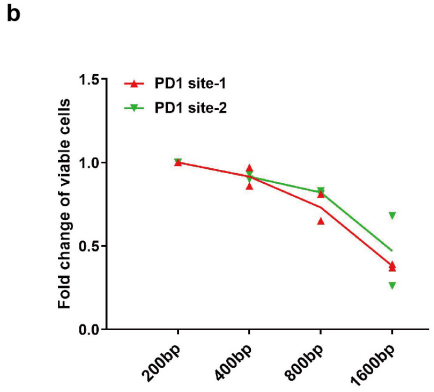

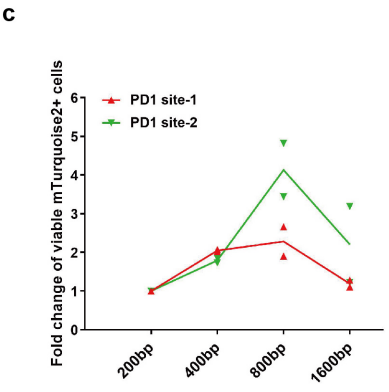

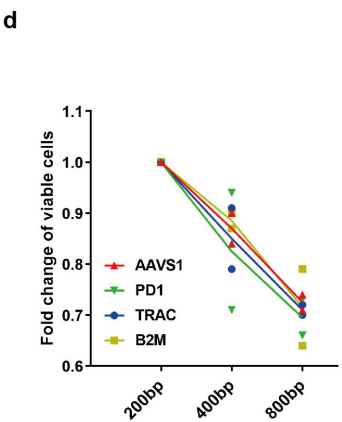

Supplementary figure 2 Comparison of recombination efficiency and cell viability among templates with different length of homology arms

The sequence of fluorescent protein mTurquoise2 was used as a target to compare different homology arm lengths in a-c. a-c, Recombination efficiency (a) and numbers of all viable cells (b) and viable mTurquoise2+ cells (c) were detected 7 days after electroporation using equal molar mTurquoise2 templates with different homology arm lengths. d, Number of all viable cells was enumerated 7 days after electroporation using equal molar CAR templates with different homology arm lengths. All the experiments were performed in two independent healthy donors. Mean value is shown in all the figures.

Supplementary figure 3

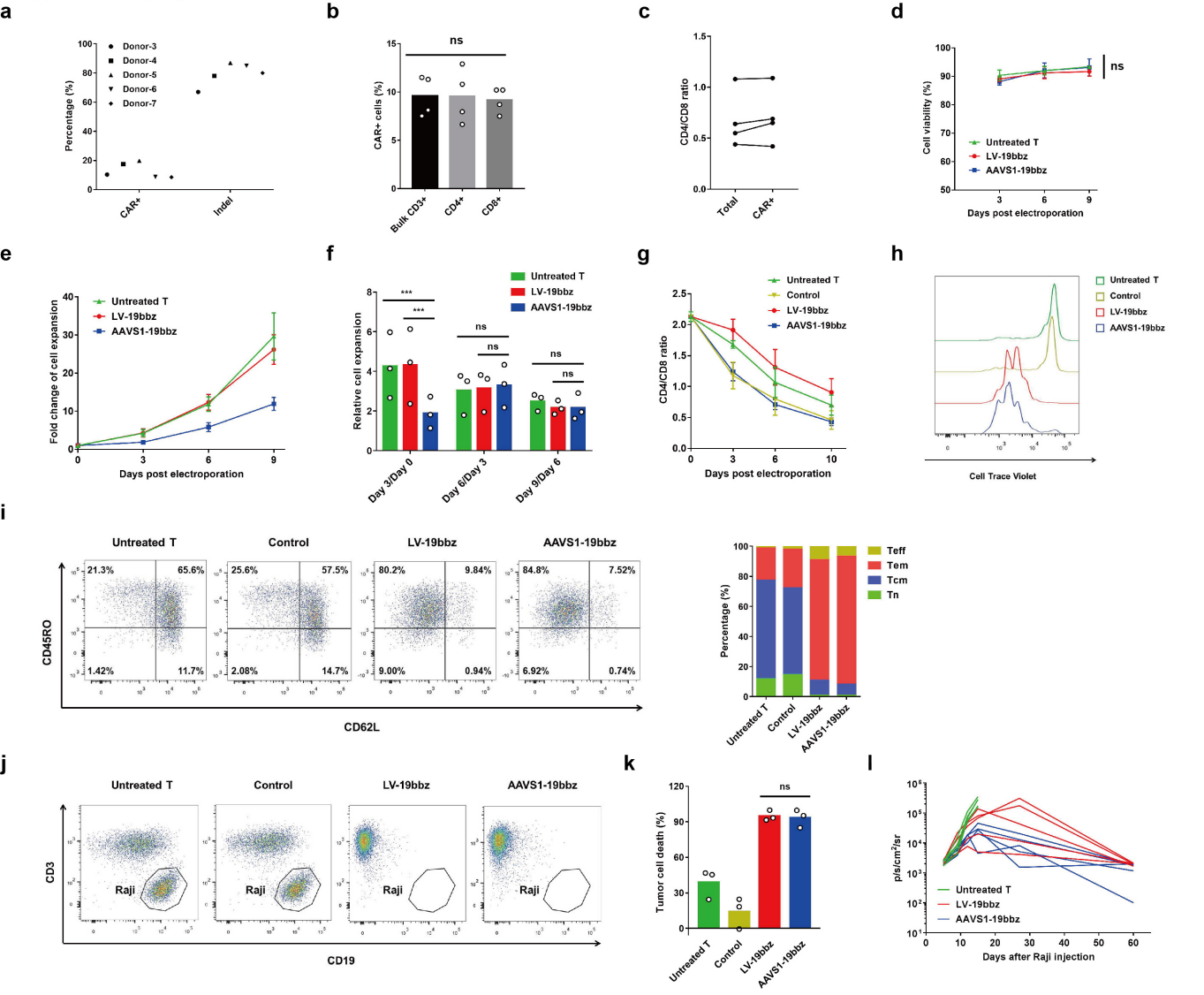

Supplementary figure 3 Non-viral *AAVS1*-integrated CAR T cells behave comparably to conventional CAR T cells

a, Percentages of CAR integration and *AAVS1* indels in total T cells were detected 7 days after electroporation in five representative healthy donors. b, Percentages of CAR integration in CD3+, CD4+ and CD8+ cells determined 7 days after electroporation (n=4 independent healthy donors). c, Comparison of CD4/CD8 ratio between total and CAR+ cells (n=4 independent healthy donors). d, Cell viability detected by trypan blue staining on indicated days post electroporation. Data are mean ± SEM (n=3 independent healthy donors). e-f, Absolute (e) and relative (f) rates of T cell growth *in vitro* (n=3 independent healthy donors). Data are mean ± SEM in e. g, Ratio of CD4+ and CD8+ cells on indicated days post electroporation. Data are mean ± SEM (n=3 independent healthy donors). h, Representative histogram showing Cell Trace Violet staining of T cells after co-culture with mitomycin C-treated Raji cells for 5 days. i, Representative flow cytometry plots showing CD45RO/CD62L expression in T cells after 24 hours co-culture with Raji cells. The T cell subset differentiation is shown at right. j, Representative flow cytometry plots showing lysis of Raji cells following 18 hours co-culture. k, The percentage of Raji tumor cell death detected by flow cytometry-based cytotoxicity assay (n=3 independent healthy donors). l, Bioluminescence kinetics of Raji tumor cell growth in NSG mice following different treatments (n=5). Control samples were electroporated the same as AAVS1-19bbz cells except without sgRNA addition. CD3+ (Untreated T, Control) or CD3+/CAR+ (LV-19bbz, AAVS1-19bbz) gated cells are analyzed in h, i. Mean value is shown in b, f, k. P values are calculated by one-way ANOVA (b, k) or two-way ANOVA (d, f).

Supplementary figure 4

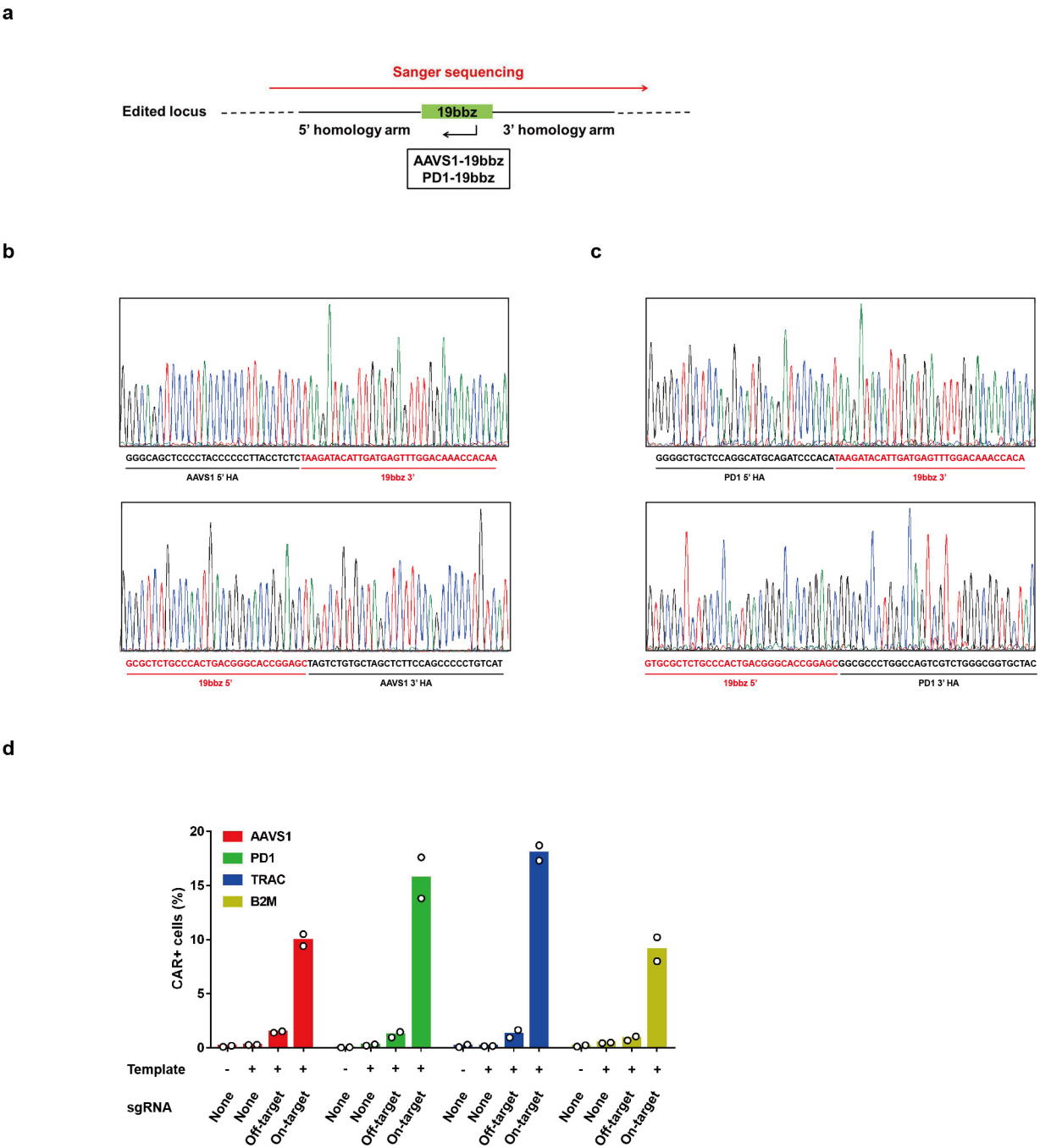

Supplementary figure 4 Site-specific integration of CAR cassette

a, For the samples of AAVS1-19bbz and PD1-19bbz, CAR+ cells were sorted by fluorescence-activated cell sorting (FACS). Genomic DNA was used as template to amplify PCR products across the homology arms. Sanger sequencing was performed from end to end, outside of homology arms. b-c, Sequences of 5' and 3' junction sites between the homology arm and CAR cassette at the *AAVS1* (b) and *PD1* (c) locus. d, Non-specific integration of CAR elements was tested 7 days after electroporation by using different combinations of DNA template and sgRNA (n=2 independent healthy donors). For the groups of AAVS1, PD1 and TRAC templates, one B2M sgRNA with high cleavage efficiency was used as off-target sgRNA. For the B2M template group, one TRAC sgRNA with high cleavage efficiency was used as off-target sgRNA. The off-target groups were designed to detect non-targeted integration under a hypothesized condition that sgRNA had very high off-target cleavage efficiency. Mean value is shown in d.

Supplementary figure 5

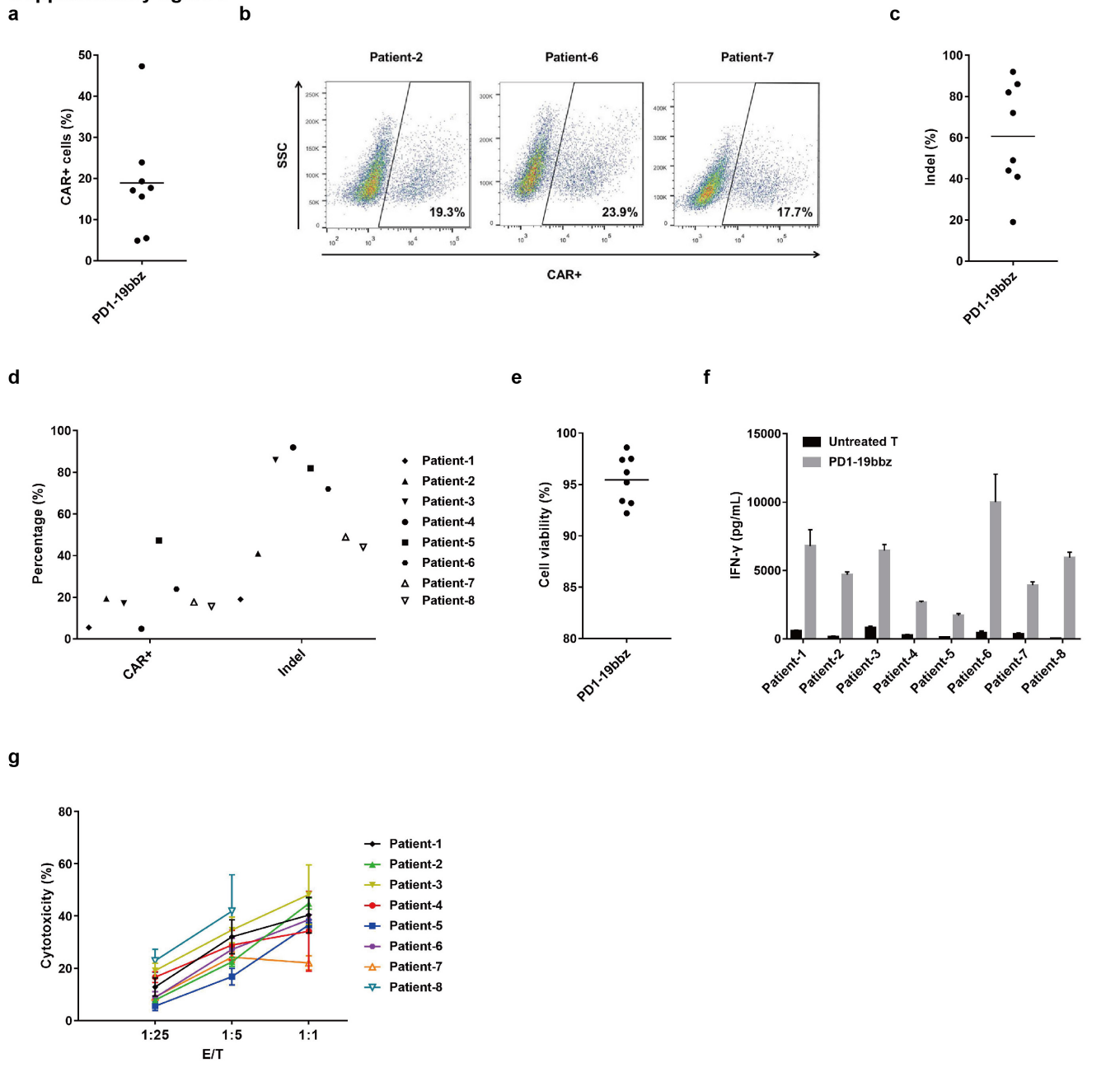

Supplementary figure 5 ***In vitro*** **evaluation of non-viral *PD1*-targeted CAR T cell products**

a, Percentage of CAR+ cells in the final products of eight r/r B-NHL patients. b, CAR expression determined in three representative patient donors. c-d, Percentages of CAR integration (d) and *PD1* indels (c, d) in the final products. e, Cell viability of the final products detected by trypan blue staining. f, IFN-γ secretion measured by ELISA in the supernatant after co-culture with Nalm-6 cells for 18-24 hours. Data are mean ± SD (n=3 technical replicates). g, *In vitro* cytotoxicity against Nalm-6 cells determined using LDH assay. E/T, effector/target. Data are mean ±SD (n=3 technical replicates). Mean value is shown in a, c, e.

Supplementary figure 6

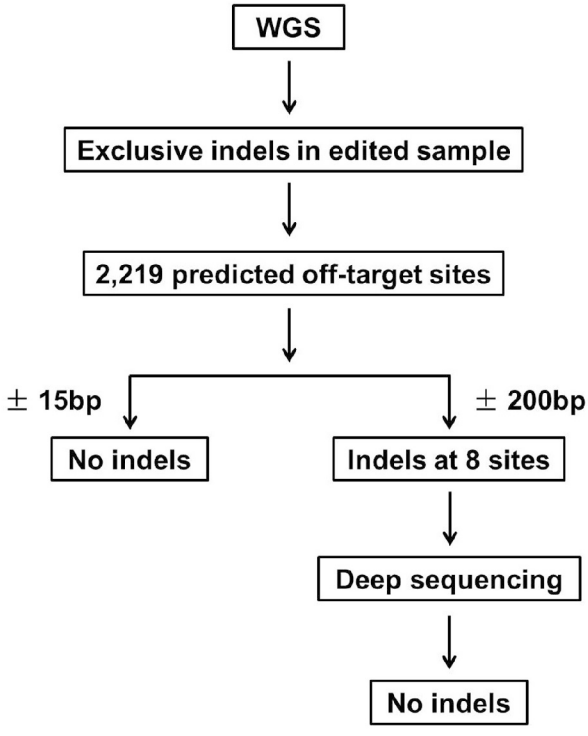

Supplementary figure 6 Off-target detection in non-viral *PD1*-integrated CAR T cells by WGS and deep sequencing

The genomic DNA of untreated T cells and the infusion product of patient-2 was subjected to 100× whole genome sequencing (WGS). A total of 2,219 potential off-target sites (not including those around the on-target site) were predicted by Cas-OFFinder and compared with exclusive indels in the edited sample by bioinformatics. No indel events were detected within 15bp upstream and downstream (±15bp) of the sites. Indels were found within 200bp upstream and downstream (±200bp) of eight sites. Deep sequencing was then performed to validate these indel events. While no indels were detected at five sites, indels at the other three sites were variances of one unit length on nucleotide repeats and thus were not considered to be true off-target events.

Supplementary figure 7

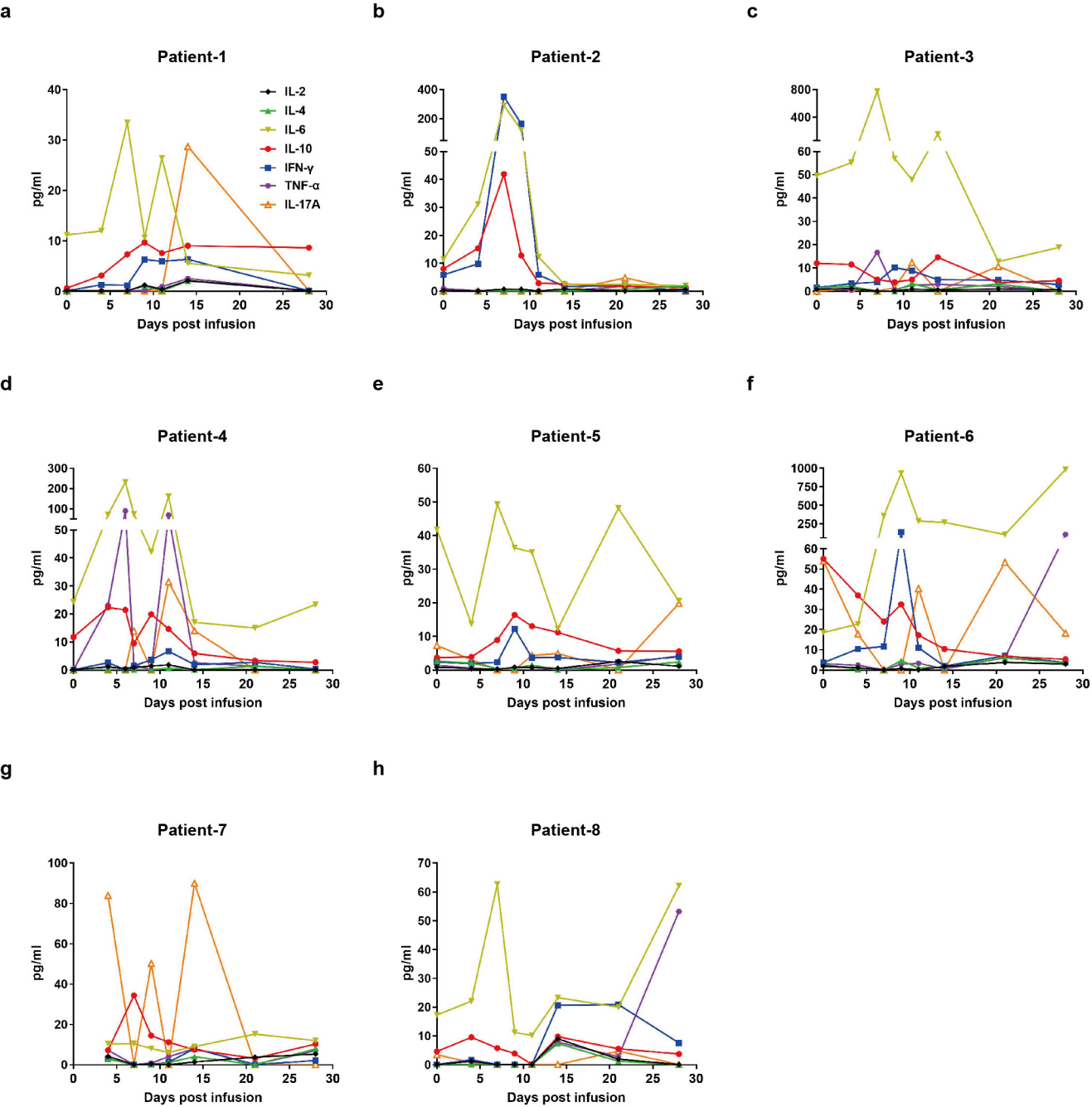

Supplementary figure 7 Serum cytokine profiles in r/r B-NHL patients after treatment of non-viral *PD1*-targeted CAR T cells

a-h, Serum cytokines including IL-2, IL-4, IL-6, IL-10, IFN-γ, TNF-α and IL-17A were assessed in eight r/r B-NHL patients on indicated days after infusion.

Supplementary figure 8

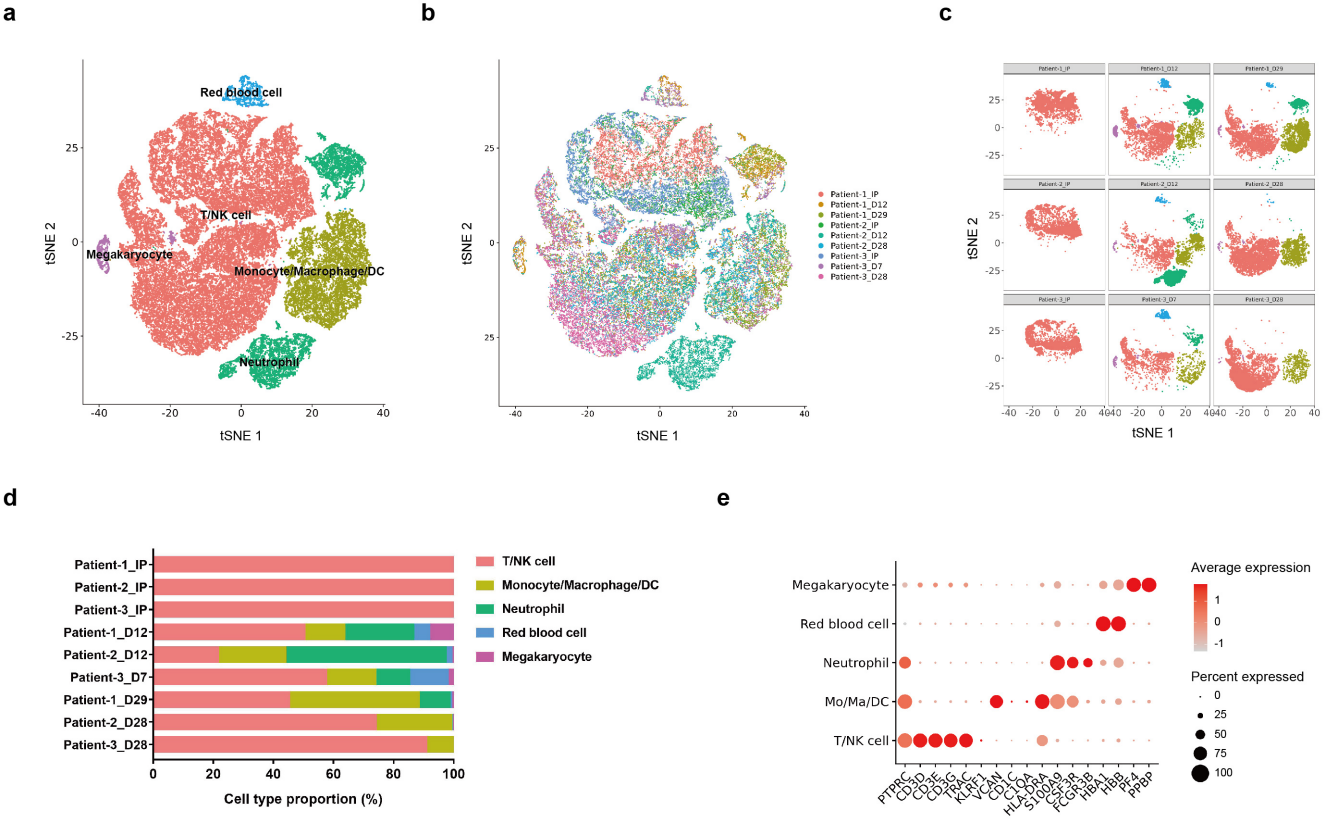

Supplementary figure 8 Overview of the single-cell landscape

a-b, Overview of the 54,774 cells that passed QC for single-cell analysis. Cells are color coded by cell type (a) and patient sample (b), respectively, in t-distributed stochastic neighbor embedding (tSNE) plots. c, tSNE plot showing cell clusters in each sample. d, Proportion of cell types in each patient sample. e, Bubble heat map showing marker gene expression for different cell types.

Supplementary figure 9

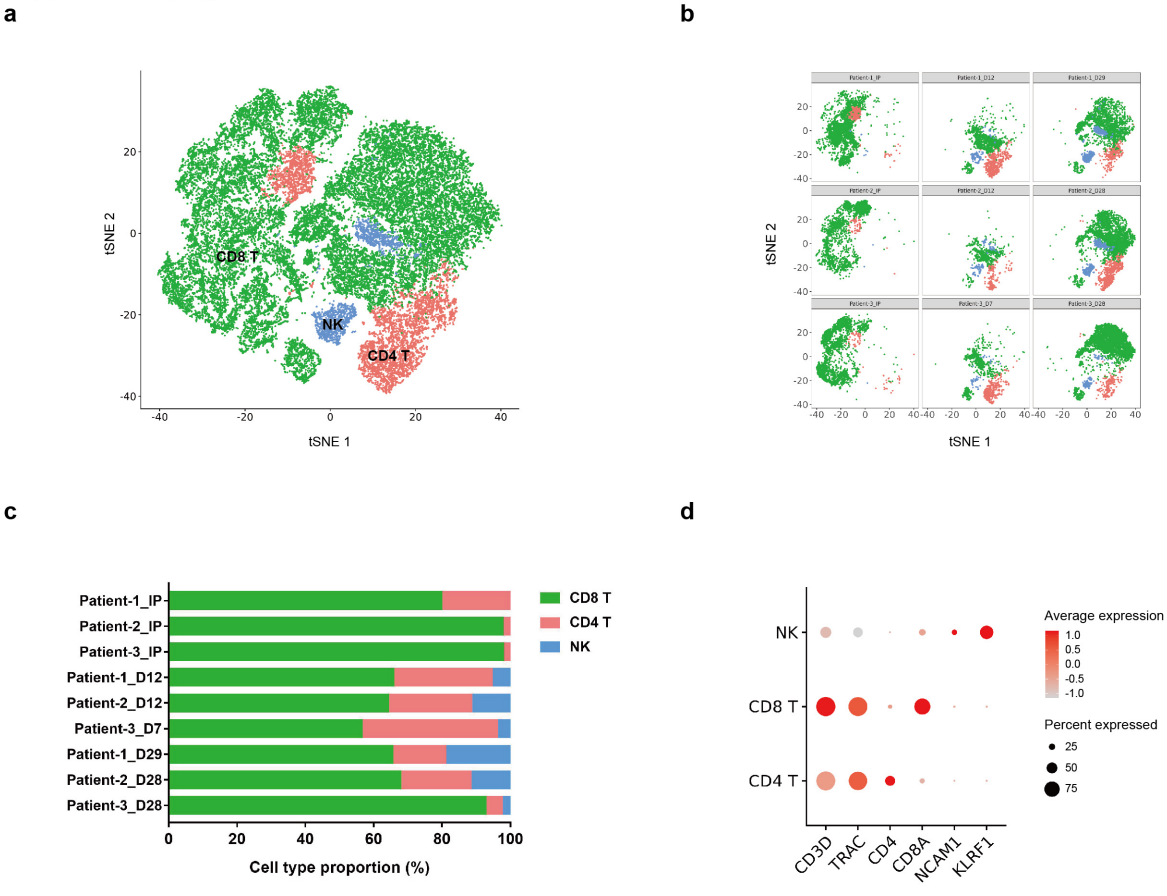

Supplementary figure 9 Landscape of T/NK cell types in single-cell analysis

a, Overview of the 36,201 cells in the T/NK cell cluster. Cells are color coded by cell type in the tSNE plot. b, tSNE plot showing subtypes in the T/NK cell cluster in each patient sample. c, Proportion of subtypes in the T/NK cell cluster in each sample. d, Bubble heat map showing marker gene expression for different subtypes in the T/NK cell cluster.

Supplementary figure 10

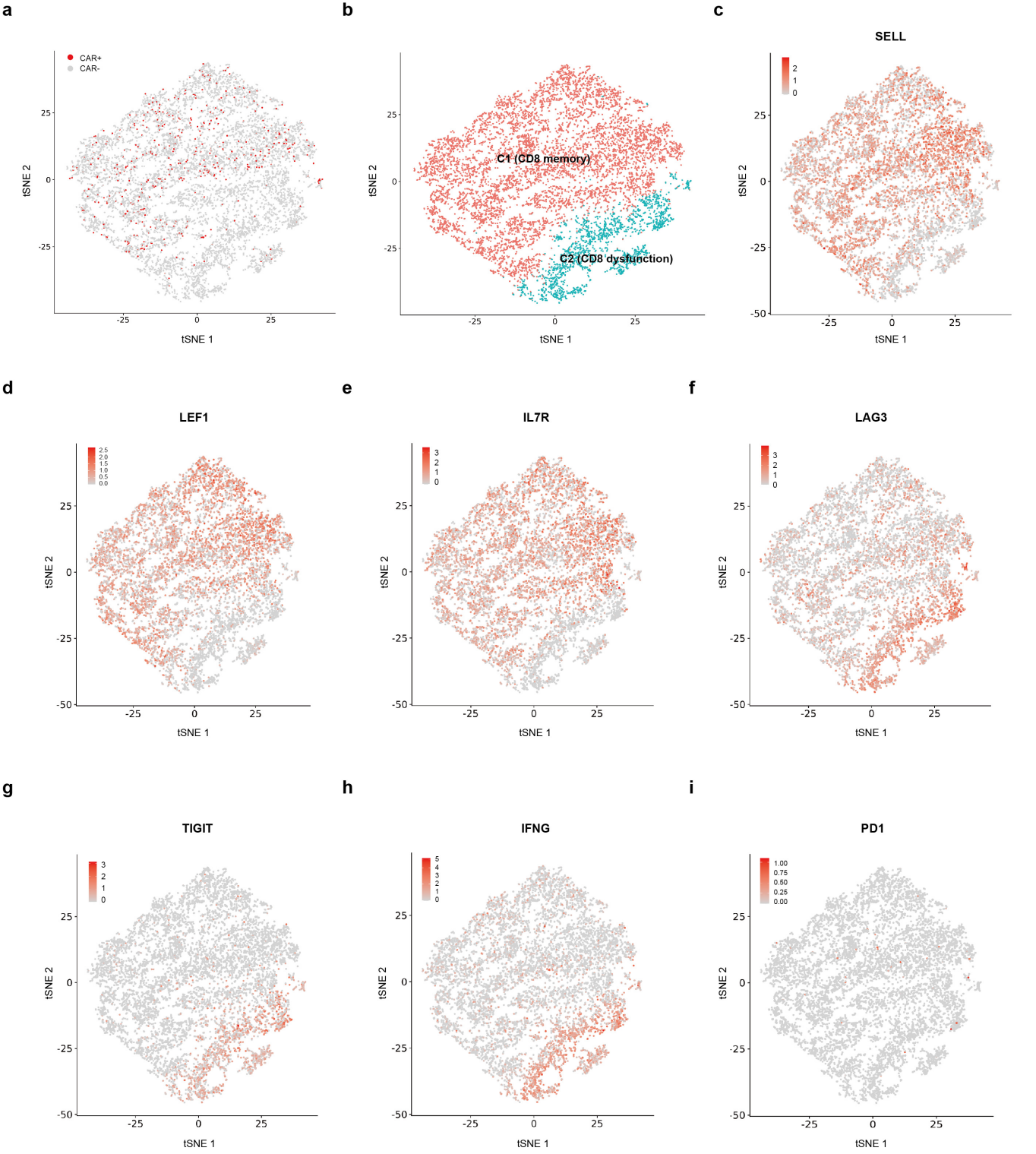

Supplementary figure 10 Single-cell analysis of non-viral *PD1*-integrated CAR T cell products

CD8+ T cells were analyzed in the infusion products of three patients. a, Distribution of CAR+ and CAR- cells in the tSNE plot. b, tSNE plot showing two clusters in the infusion products. C1 and C2 were generated by clustering CD8 memory and dysfunction marker genes, respectively. c-e, Expression of representative CD8 memory genes (SELL, LEF1, IL7R) in the tSNE plots. f-h, Expression of representative CD8 dysfunction genes (LAG3, TIGIT, IFNG) in the tSNE plots. i, Expression of PD1 in the tSNE plot.

Supplementary figure 11

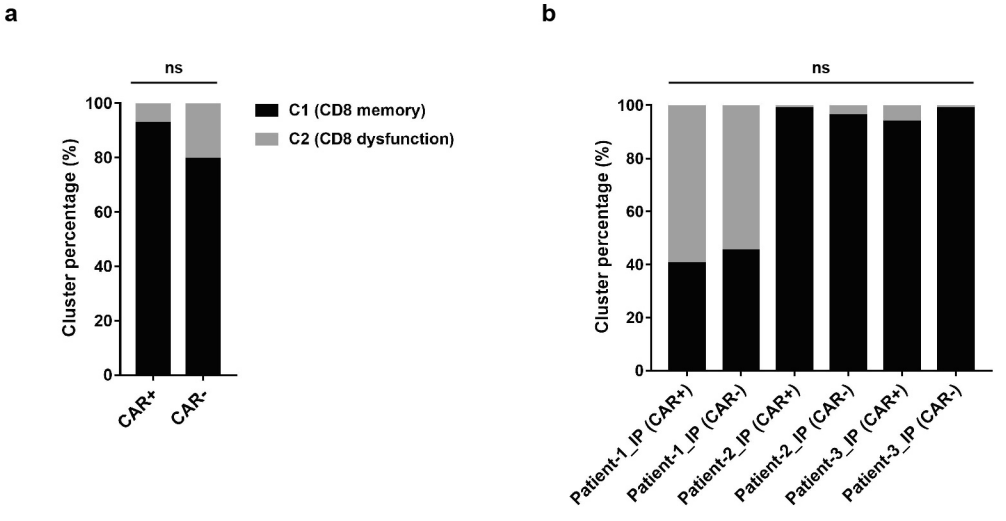

Supplementary figure 11 Proportion of CD8 memory and dysfunction clusters in infusion products

a-b, Comparison of C1 and C2 proportion between CAR+ and CAR- cells in mixed (a) and individual (b) samples of infusion products. P values are calculated by two-way ANOVA.

Supplementary figure 12

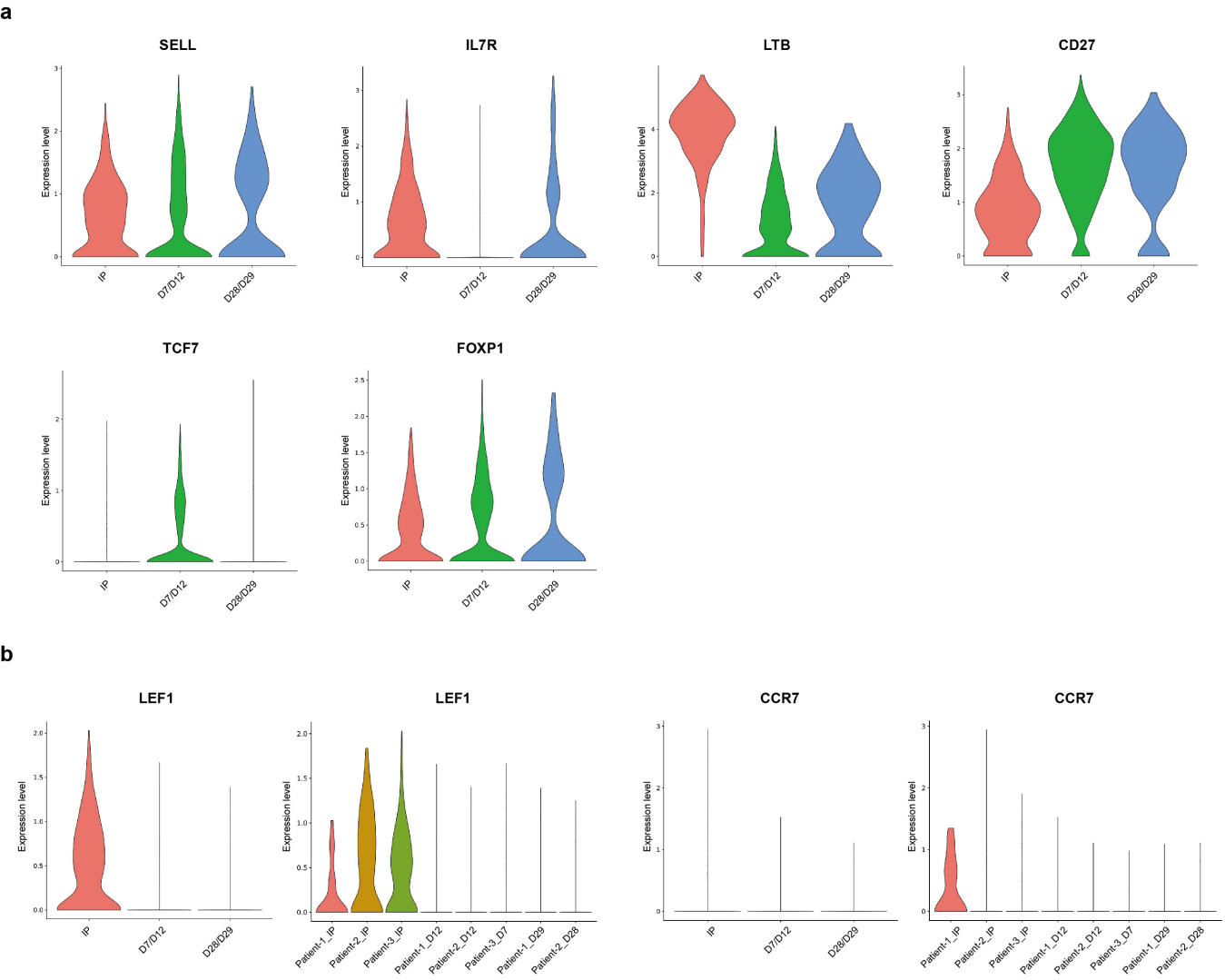

Supplementary figure 12 Expression of CD8 memory genes in non-viral *PD1*-targeted CAR T cells before and after infusion

a-b, Violin plots showing the expression of memory genes in CD8+/CAR+ cells from three patients before and after infusion. Data of mixed (a, b) and individual (b) samples are shown, respectively. The data of patient-3 sample after 28 days treatment is excluded from mixed samples and not shown individually due to an unreliable low CAR+ cell number.

Supplementary figure 13

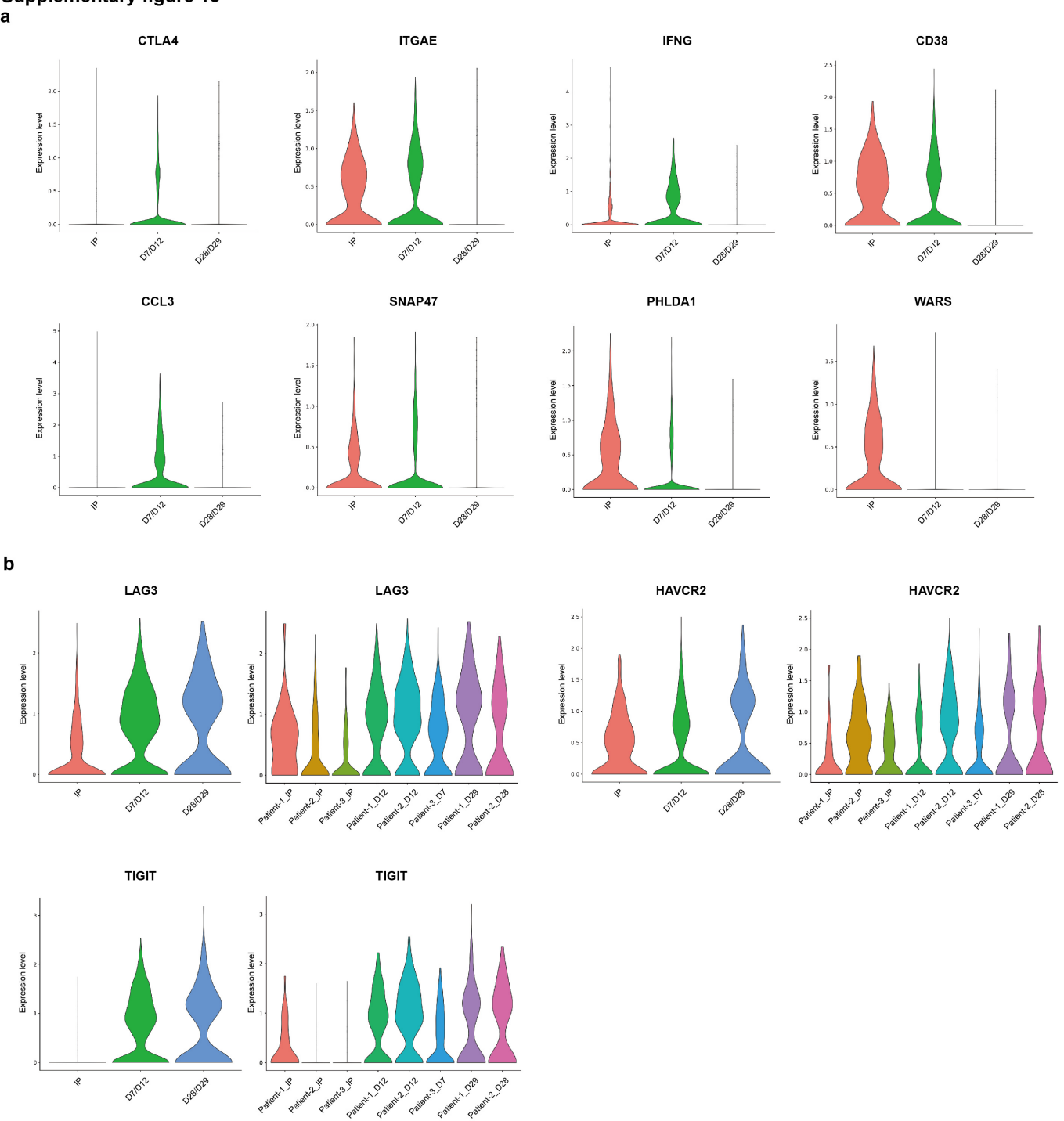

Supplementary figure 13 Expression of CD8 dysfunction genes in non-viral *PD1*-targeted CAR T cells before and after infusion

a-b, Violin plots showing the expression of dysfunction genes in CD8+/CAR+ cells from three patients before and after infusion. Data of mixed (a, b) and individual (b) samples are shown, respectively. The data of patient-3 sample after 28 days treatment is excluded from mixed samples and not shown individually due to an unreliable low CAR+ cell number.

Supplementary figure 14

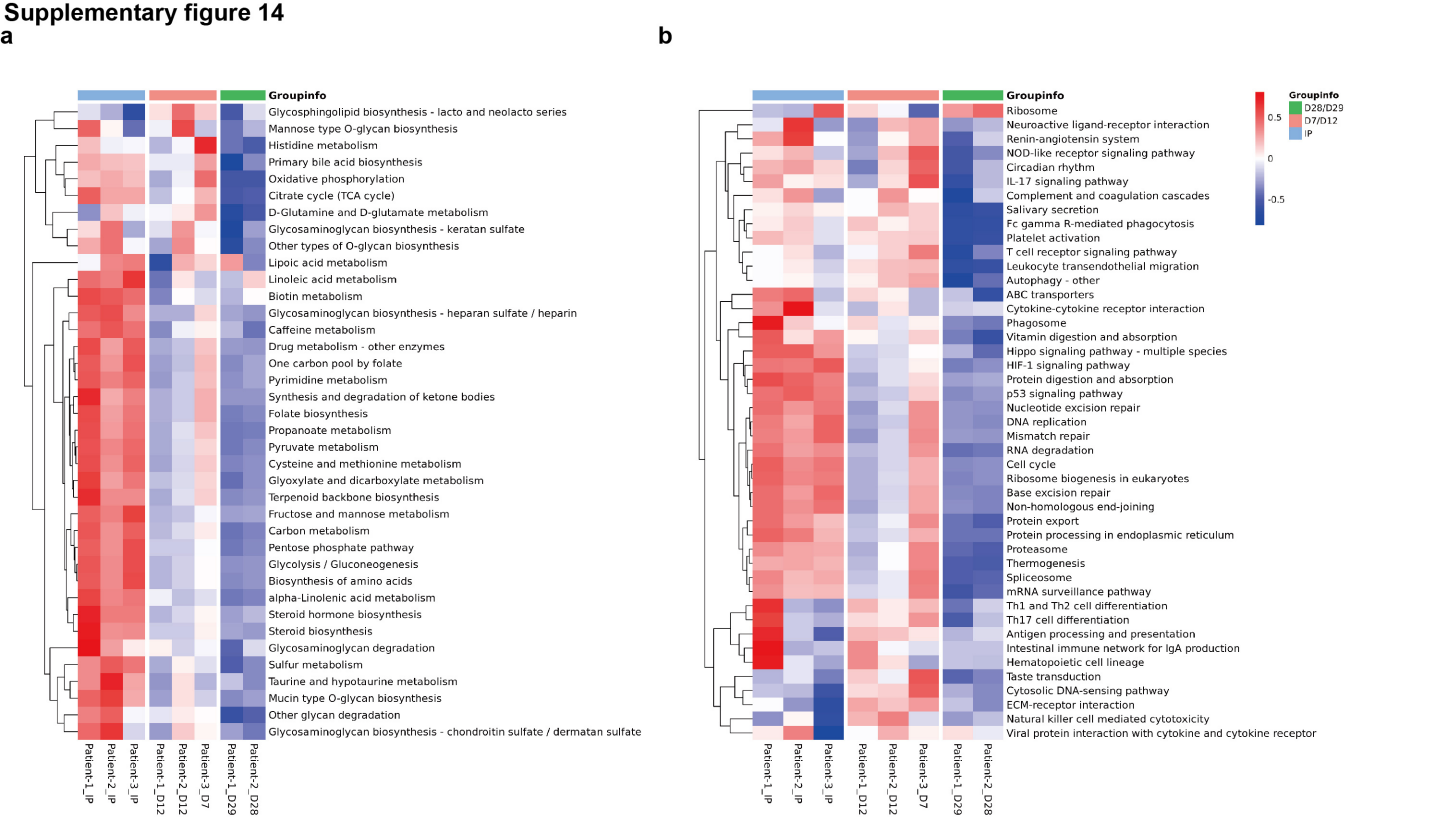

Supplementary figure 14 Gene set enrichment analysis in non-viral *PD1*-integrated CAR T cells before and after infusion

a-b, Metabolism (a) and other (b) pathway activities were scored by gene set enrichment analysis (GVSA) using the quantitative set analysis for gene expression (QuSAGE) method in three patient samples before and after infusion. The data of patient-3 sample after 28 days treatment is excluded from mixed samples and not shown individually due to an unreliable low CAR+ cell number.

Table 1 Patient characteristics, clinical responses and adverse events

Patient	Sex	Age (years)	Lymphoma type	Number of prior lines of therapy[a]	Disease stage	Lymphoma status[b]	CAR+ cell dose (/kg)	Best response (duration in months)[c]	CRS	Neurological toxicity
Patient-1	M	44	GCB DLBCL	5	IV	Refractory	0.56×10^6	CR (9+)	Grade 1	None
Patient-2	M	53	Non-GCB DLBCL	4	IV	Refractory	2.04×10^6	CR (7+)	Grade 1	None
Patient-3	M	59	GCB DLBCL	3	IV	Refractory	1.95×10^6	PR (1)	Grade 1	None
Patient-4	M	46	Non-GCB DLBCL	10	IV	Relapsed within 6 months after ASCT	0.8×10^6	CR (4+)	None	None
Patient-5	F	43	B-LBL	4	IV	Refractory	0.76×10^6	CR (4+)	None	None
Patient-6	F	64	Non-GCB DLBCL	4	IV	Refractory	2.35×10^6	CR (3+)	Grade 2	None
Patient-7	F	62	GCB DLBCL	1	III	Refractory	2.15×10^6	CR (3.5+)	None	None
Patient-8	F	51	FL	6	IV	Refractory	1.9×10^6	CR (3+)	None	None

ASCT, autologous stem cell transplant; B-LBL, B-cell lymphoblastic lymphoma; CR, complete remission; DLBCL, diffuse large B cell lymphoma; F, female; FL, follicular lymphoma; GCB, germinal center B cell; M, male; PD, progressive disease; PR, partial remission.[a]All prior lines of therapy for each patient are listed in Supplementary table 4 [b]Disease was defined as refractory if a patient did not achieve partial or complete remission after the most recent chemotherapy. [c]Best response was defined as the best response that a patient achieved after CAR T cell infusion. [d]Response duration is the time from the first documentation of response, until progression, initiation of off-study treatment or the last documentation of ongoing response. The + symbol indicates an ongoing response.

Table S1 Deep sequencing analysis of 8 off-target (OT) sites detected by WGS

Number	Chrom	Predicted OT pos	Indel pos	Distance (bp)	On-target seq	Predicted OT seq	Strand	Function	Mutation type	Validated by deep seq	Nucleotide repeats
1	chr15	34428733	34428916	182	CGACTGGCCAGGGCGCCTGTGGG	CGATAGGCCAGGGCGCCT-GCAG	-	intergenic	1-5 bp deletion 1 bp insertion	Yes	AAAAAAAAAAAAAAAAAAAA
2	chr15	34574943	34575106	162	CGACTGGCCAGGGCGCCTGTGGG	CGATAGGCCAGGGCGCCT-GCAG	-	intergenic	NA	No	NA
3	chr15	34574943	34575120	176	CGACTGGCCAGGGCGCCTGTGGG	CGATAGGCCAGGGCGCCT-GCAG	-	intergenic	NA	No	NA
4	chr17	47703037	47702993	43	CGACTGGCCAGGGCGCCTGTGGG	CGAAGGGACAGGGGGTCTGTGAG	+	intronic	2 bp deletion	Yes	GGGGGGGGG
5	chr2	72911968	72912124	155	CGACTGGCCAGGGCGCCTGTGGG	TGAGTGTCTAGGGGGCCTGTAGG	+	intergenic	NA	No	NA
6	chr21	13246921	13246759	161	CGACTGGCCAGGGCGCCTGTGGG	CGTCTAGCCAGGGAGCATCTCAG	-	intergenic	4 bp insertion	Yes	TGTGTGTGTGTGTGTGTGTGTGTGTGTGTG
7	chr3	187139213	187139074	138	CGACTGGCCAGGGCGCCTGTGGG	GCAGAGGCCAGGGCGCCGGTAAG	-	intronic	NA	No	NA
8	chr9	131301652	131301813	160	CGACTGGCCAGGGCGCCTGTGGG	CGCCTGGCCCGGGAAGCTGTGGG	-	intronic	NA	No	NA

Table S2 Deep sequencing analysis of top 29 off-target sites predicted by the Benchling CRISPR tool

Site	Chrom	Position	Target sequence	PAM	Strand	Mismatch
On-target	chr2	241858825	CGACTGGCCAGGGCGCCTGT	GGG	+	0
Off-target 1	chr12	590629	CCACTGCCCAGGGCGCCTGG	AAG	+	3
Off-target 2	chr3	135323926	CAACTGGCCAGGGCACCTAT	GAG	+	3
Off-target 3	chr1	1088609	CCACCGGCCAGGGCGCCTTT	AAG	+	3
Off-target 4	chr8	53878623	GGACTGGCCAGTGCGGCTGT	AGG	−	3
Off-target 5	chr15	78526890	AGACTGGCCAGGGAGTCTGT	GAG	−	3
Off-target 6	chr3	123344000	GGACTGGCCAAGGAGCCTGT	AGG	−	3
Off-target 7	chr21	43988998	CGTGTGGCCAGGGGGCCTGT	GAG	+	3
Off-target 8	chr11	62855728	TGCCTGGCCAGGGCGACTGG	CGG	−	4
Off-target 9	chr9	92171112	GGCCTGGCCAGGGCGGCTGG	GGG	−	4
Off-target 10	chr11	1153416	GGCCTGGCCAGGGCCCCTGC	TGG	+	4
Off-target 11	chr14	92376556	GGGCTGGCCAGGGCCCCTGA	GGG	+	4
Off-target 12	chr11	36455288	GGCCTGGCCAGGGAGCCTGG	GAG	+	4
Off-target 13	chr1	19454074	AGAGTGGCCAGGGCTCCTGG	AGG	+	4
Off-target 14	chr1	3982141	TGTCTGGCCAGGGTGCCTGC	TGG	+	4
Off-target 15	chr10	133474998	AGACAGGCCAGGGCACCTGC	AGG	−	4
Off-target 16	chr13	113104005	CTGCTGGCCAGGGCGGCTGC	AGG	−	4
Off-target 17	chr1	6103274	AGCCTGGCCAGGGCTCCTTT	GGG	−	4
Off-target 18	chr16	53503575	CAATTGGCCAGGGCGTCTGC	CAG	+	4
Off-target 19	chr5	758609	TGCCTGGCCATGGCGCCTGC	AGG	−	4
Off-target 20	chr9	109891067	CCCCTGGCCAGGGTGCCTGG	AGG	+	4
Off-target 21	chr8	11549226	GGACTGACCAGGGAGCCTGC	AGG	+	4
Off-target 22	chr2	239056117	CGCCAGGCCAGGGCGCCAGG	CAG	+	4
Off-target 23	chr2	229943631	CCACGGGCCAGGGCTCCTGA	CAG	−	4
Off-target 24	chr10	102415823	GGACTGGGCAGGGCACCTGG	AGG	−	4
Off-target 25	chr7	149765282	CCCCTGGCCAGCGCGCCTGG	CGG	−	4
Off-target 26	chr6	35078996	AGGCTGGCCAGGGCTCCAGT	GAG	−	4
Off-target 27	chr1	153642303	CCCCTGGCCAGGGCCCCTAT	GGG	−	4
Off-target 28	chr2	201929252	CCACAGGCCAGGGTGCCTGG	AAG	+	4
Off-target 29	chr5	1104177	TGACTGCCCAGGGCGTCTCT	GAG	+	4

Table S3 Infusion products of non-viral *PD1* integrated CAR T cells

Patient	Weight (kg)	CAR+ cell dose (/kg)	Total cell number	CAR+ (%)	Viability (%)	CD4/CD8 ratio
Patient-1	62	0.56×10^{6}	6.32×10^{8}	5.49	96.2	0.75
Patient-2	89	2.04×10^{6}	9.41×10^{8}	19.3	97.5	0.15
Patient-3	75	1.95×10^{6}	8.55×10^{8}	17.1	98.6	0.35
Patient-4	70	0.8×10^{6}	1.15×10^{9}	4.87	95.2	1.11
Patient-5	63	0.76×10^{6}	1.01×10^{8}	47.3	93.4	0.01
Patient-6	60	2.35×10^{6}	5.90×10^{8}	23.9	92.2	0.50
Patient-7	59	2.15×10^{6}	7.17×10^{8}	17.7	93.2	0.18
Patient-8	42	1.9×10^{6}	5.12×10^{8}	15.6	97.4	0.30

Table S4 Prior lines of therapy for each patient

Patient	Number of prior lines of therapy	Prior therapies
Patient-1	5	R-CHOP Sintilimab + ICE + R-Gemox + Chidamide R-Gemox + Chidamide Radiation therapy Rituximab + Lenalidomide + Chidamide
Patient-2	4	R-COP RCD Lenalidomide R-DA-EPOCH
Patient-3	3	R-CHOP R2-CHOP R-CHOPE
Patient-4	10	R2-CHOP Rituximab + Lenalidomide Rituximab Rituximab+ Ibrutinib+ EPOCH R-Hyper-CVADA Rituximab+ Ibrutinib+ Hyper-CVADA Rituximab+ Ibrutinib ASCT SMART Brentuximab vedotin + Ibrutinib + CHOP
Patient-5	4	R-VDP Hyper-CVADA Hyper-CVADB MTX + Asparaginase + DXM
Patient-6	4	R-CHOP R-GDP R-CHOP R2-DA-EPOCH
Patient-7	1	R-CHOP
Patient-8	6	BR C1 BR C2 BR C3 BR C4 R2-CHOP R-GDP

ASCT: autologous stem cell transplant; BR: bendamustine, rituximab; CHOP: cyclophosphamide, adriamycin, vincristine, prednisone; CHOPE: cyclophosphamide, adriamycin, vincristine, prednisone, etoposide; COP: cyclophosphamide, vincristine, prednisone; DA: dose adjustment; DXM: dexamethasone; EPOCH: etoposide, prednisone, vincristine, cyclophosphamide, doxorubicin; GDP: gemcitabine, dexamethasone, cisplatin; Hyper-CVADA: cyclophosphamide, vincristine, doxorubicin, dexamethasone; Hyper-CVADB: methetrexate, cytarabine; ICE: ifosfamide, carboplatin, etoposide; MTX: methotrexate; R: rituximab; R2: revlimid, rituximab; RCD: rituximab, cyclophosphamide, dexamethasone; R-GemOx: rituximab, gemcitabine, oxaliplatin; SMART: simultaneous modulated accelerated radiotherapy; VDP: vincristine, daunorubicin, prednisone.

Table S5 Summary of adverse events in the study

AE category	Toxicity	All grades	Grade 1/2	Grade 3/4
CRS	/	4	4	0
Hematologic	Decrease in white blood cells	17	9	8
	Increase in white blood cells	1	1	0
	Decrease in lymphocytes	12	1	11
	Decrease in platelet	5	1	4
	Decrease in neutrophil	19	5	14
	Hypoalbuminemia	2	2	0
	Anaemia	5	1	4
	Low fibrinogen	1	1	0
Electrolyte	Hypocalcemia	4	4	0
	Alkaline phosphatase	1	1	0
Metabolic	Hypertriglyceridemia	4	4	0
Gastrointestinal	Abdominal distention	1	1	0
	Abdominal distention and nausea	1	1	0
	Nausea	1	1	0
	Dysphagia	1	1	0
	Throat discomfort	2	2	0
	Abdominal aching	2	2	0
Respiratory	Cough or with expectoration	2	2	0
	Thick breathing sounds	1	1	0
Neurologic	Headache	1	1	0
	Dizzy	1	1	0
Other	Fatigue	1	1	0
	Multiple lumps	1	1	0
	Small amount of urine	1	1	0
	Left leg swell	1	1	0
	Subcutaneous mass of left elbow	1	1	0
Total		93	52	41

Figures

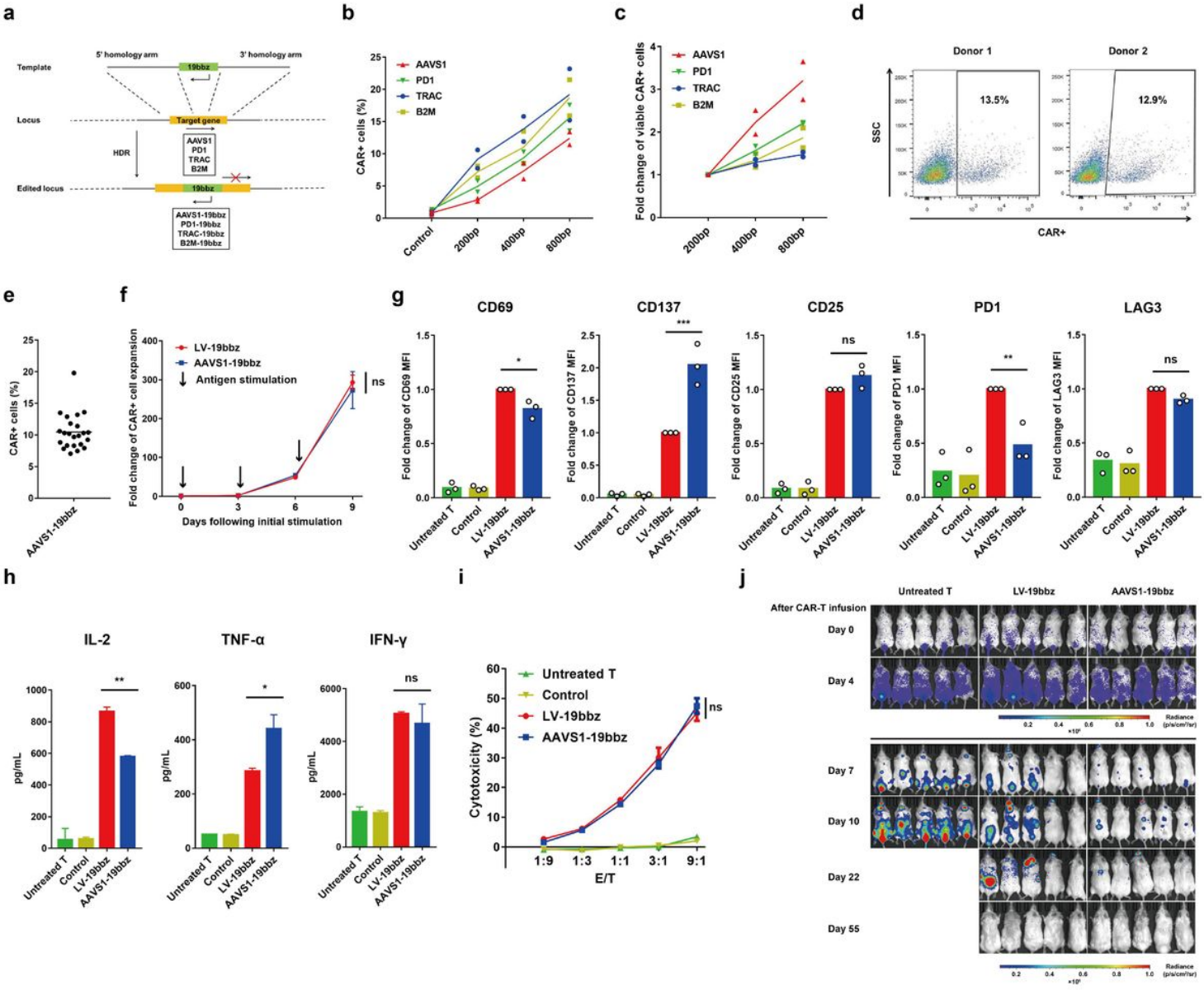

Figure 1

Non-viral AAVS1-integrated CAR T cells eliminate tumor cells as effectively as conventional CAR T cells (see Manuscript file for full figure legend)

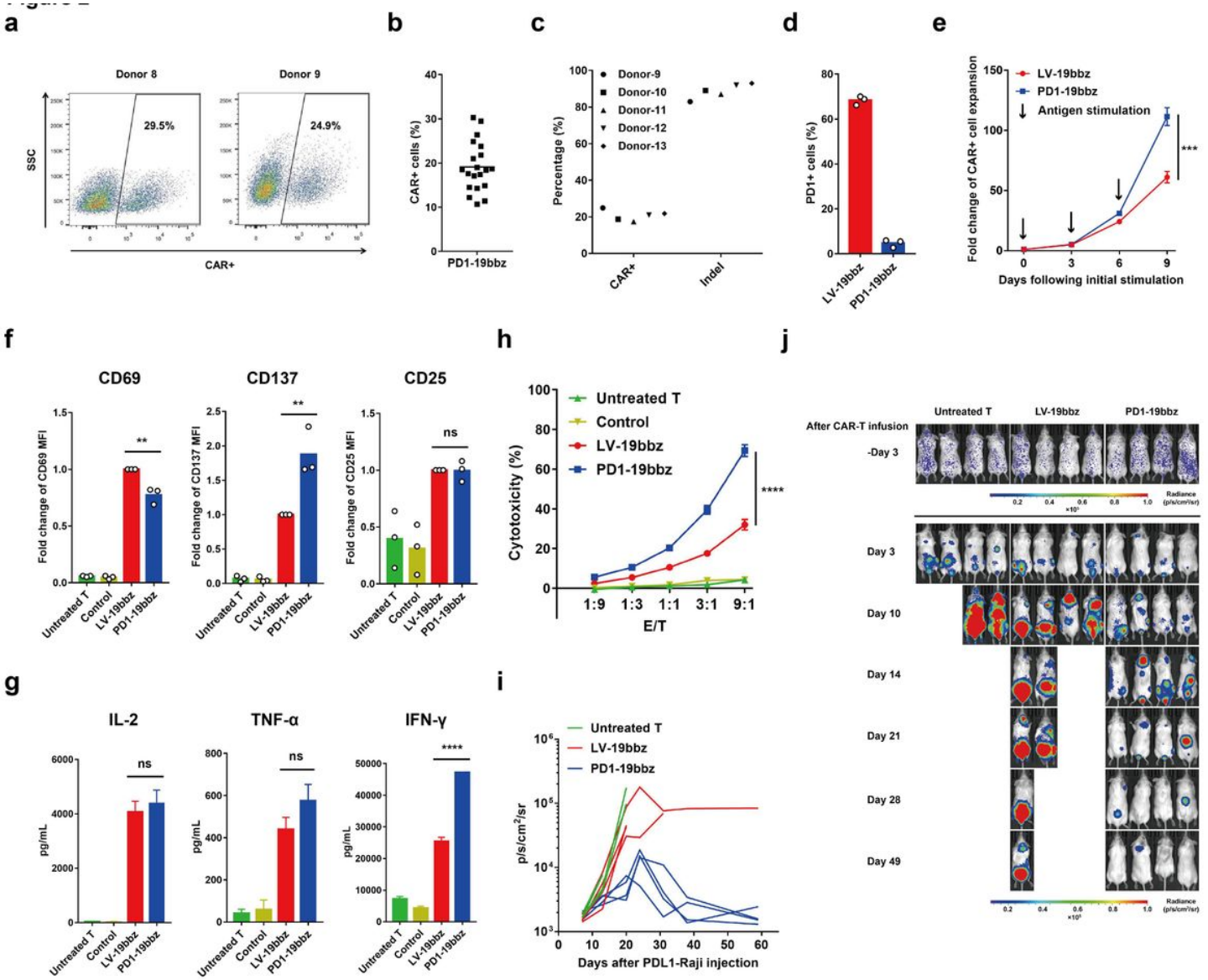

Figure 2

Non-viral PD1-integrated CAR T cells outperform conventional CAR T cells (see Manuscript file for full figure legend)

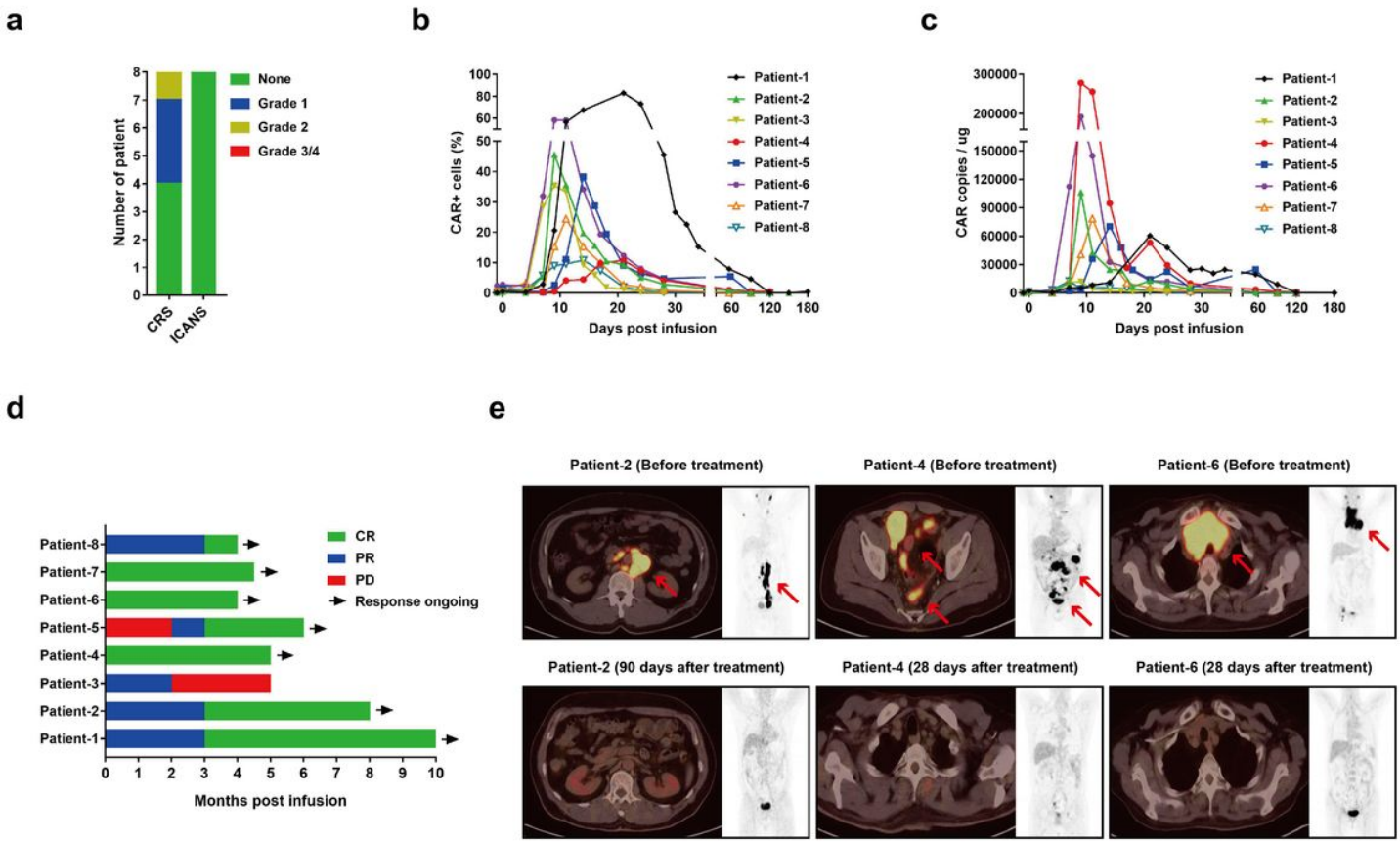

Figure 3

Non-viral PD1-integrated CAR T cells potently eliminate tumor cells in patients with r/r B-NHL without serious toxicity (see Manuscript file for full figure legend)

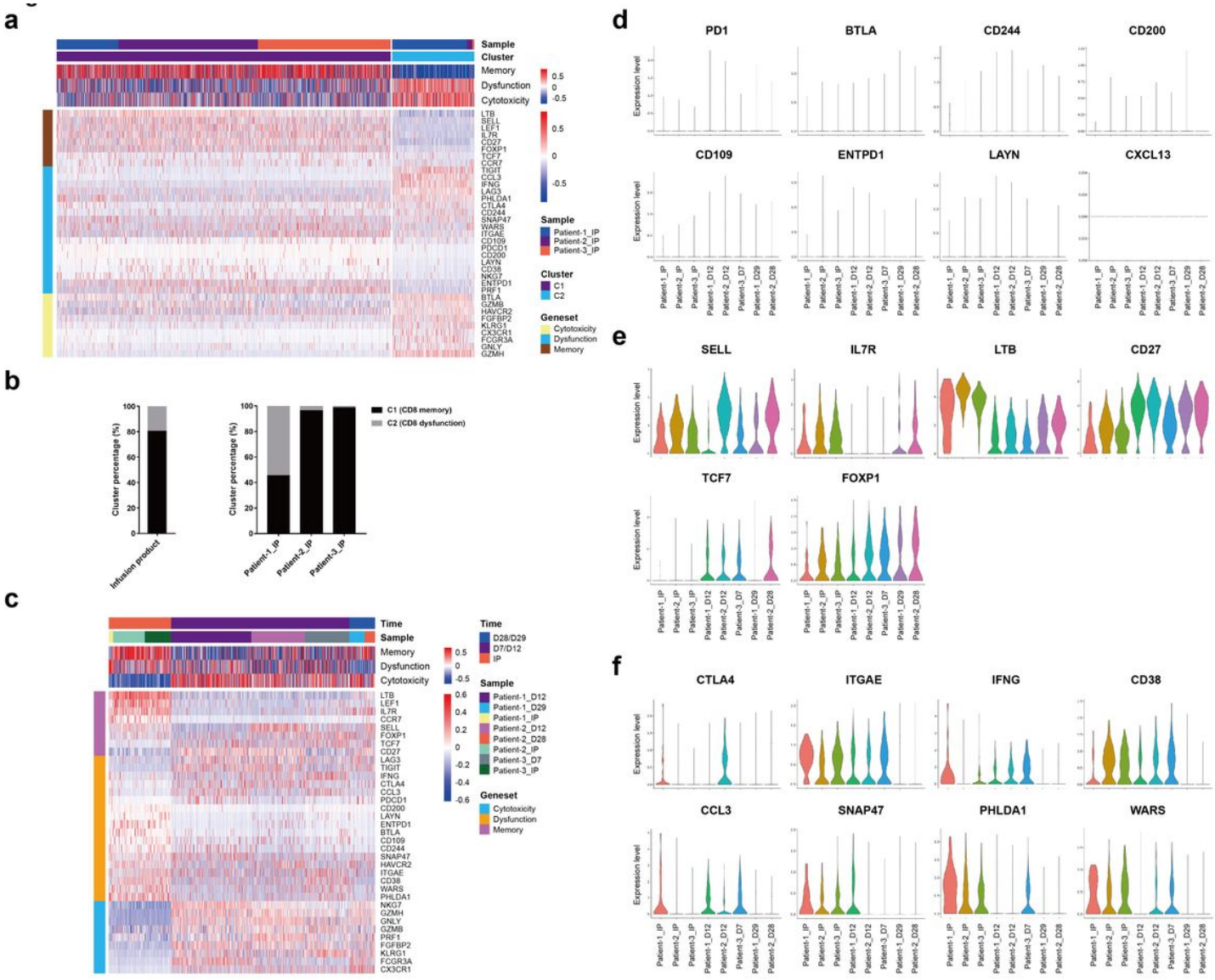

Figure 4

Single-cell RNA sequencing of non-viral PD1-integrated CAR T cells before and after infusion (see Manuscript file for full figure legend)

Supplementary Files

This is a list of supplementary files associated with this preprint. Click to download.

- TablesS1S5.pdf
- TableS6.xlsx
- TableS7.xlsx
- TableS8.xlsx
- TableS9.xlsx